

# **Mir Photo/TV Survey (DTO-1118): STS-86 Mission Report**

---



Prepared by:  
**Image Science and Analysis Group**  
**Space Science Branch**  
**Earth Science and Solar System Exploration Division**

March 4, 1998

---

## ACKNOWLEDGMENTS

This document was prepared by Image Science & Analysis Group (IS&AG) personnel in the Space Science Branch, Earth Science and Solar System Exploration Division. Mike Gaunce/NASA/JSC, Robert Scharf/LMES, Teresa Morris/LMES, Vince Elliott/LMES, Laura Labuda/LMES, Kevin Crosby/LMES and Jim Dragg/LMES have all made contributions to the preparation and analysis that have gone into this report. Kurt Bush/SP/LMES provided invaluable assistance in generating CAD images used in the resolution of camera field-of-view issues and crew training documents during the months leading up to STS-86. Dominic Ngan/Rockwell-Downey provided much of the information on the Mir Station configuration changes. Thanks are given to the film and video personnel in the Imagery & Publications Office/BT4 without whose help many extra hours of sorting through data would have been required. Special thanks to Judy Alexander/DF/CB/USA and Don Carico/DF/CB/USA for helping integrate DTO-1118 requirements into the crew training documentation. We would like to acknowledge the STS-86 crew for gathering the photographic and video data and the Instrumentation and Communications Officers (INCO) in Mission Control for their support in obtaining ground-controlled video. Finally, the support of the ISS Phase 1 Program is gratefully acknowledged. Many other individuals (too numerous to name) from various science, engineering, and operations groups have made contributions to the knowledge gathered and presented in this final report.

Questions about the contents of this document should be addressed to Mike Gaunce, JSC Code SN3, at 281-483-5153 or Robert Scharf, Lockheed Martin Code C23, at 281-483-2756.

---

---

## EXECUTIVE SUMMARY

NASA and the Russian Space Agency are involved in a cooperative venture in which the Shuttle will rendezvous and dock with the Mir Space Station during several missions from 1995 to 1998. These joint missions provide NASA scientists and engineers an opportunity to study the orbital, dynamic, and environmental conditions of long-duration spacecraft, as well as develop evaluation and risk mitigation techniques which have direct application to the International Space Station.

STS-86 was the Shuttle's eighth rendezvous with, and seventh docking to, the Mir. STS-86 was launched on September 25, 1997 and was docked to Mir from September 27 to October 3, 1997.

Detailed Test Objective 1118 (DTO-1118) integrates the requirements for photographic and video imagery of Mir generated by the engineering, operations, and science communities within NASA. Although mission requirements vary, the principal objectives of the DTO-1118 Mir Photo/TV Surveys are as follows:

- Study the effects of the space environment on a long-duration orbiting platform.
- Assess the overall condition of the Mir.
- Provide assurance of crew and Shuttle safety while in the proximity of the Mir Space Station.
- Analyze the dynamic effects of structures and appendages (e.g., solar array motion).
- Understand the impact of plume impingement during proximity operations.
- Evaluate the equipment and procedures used to gather survey data.

This report documents the results from STS-86 survey-related imagery analysis tasks. It is the last DTO-1118 mission analysis report for the Phase 1, Shuttle/Mir program. Support for STS-89 and STS-91 includes planning, screening, quick-look reporting, and special analysis as required. A final integrated report summarizing and integrating all analyses and assessments of the Mir survey imagery from all Shuttle/Mir missions will also be prepared. Reports of Mir photo survey and analysis activities from previous missions are listed in Section 11, References.

### Summary of Findings

As part of DTO-1118, approximately 1700 photographs and 54 hours of video of the Mir Space Station were acquired during the STS-86 mission. The significant findings from the analyses of still photography and video from this mission are as follows:

- The damage to Mir caused by the Progress collision appears limited to the surfaces and appendages of Spektr. The Spektr SP#1 received the greatest amount of damage, with sheared center support beams and a large hole through the array. SP#3 had a scrape mark and some bent supports. One radiator on the surface of the module was bent in the collision. The areas of damage are described in Section 3 and Appendix A.
-

- 
- The Spektr module was pressurized twice during the STS-86 fly-around of Mir in an attempt to detect leakage from the module. The video recorded from PLB camera D during the Mir fly-around on STS-86 provided data on seven particles which were seen moving away from Spektr between one and two minutes after the first gas release. One of these particles is also seen in the video recorded from PLB camera B. Two-dimensional analysis of the trajectories of the particles indicate multiple regions where the module may have leaks. Only one particle can be traced across the surface of the Spektr module and only for a short distance. The current analysis has not determined precise locations of origin for the particles. Additional analysis of the imagery may yield more information. The analysis and results of the assessment of Spektr venting test imagery are provided in Appendix B.
  - The overall quality of the imagery from STS-86 was excellent. The crew acquired detailed imagery using the 35 mm camera with 400 mm lens while docked and during the fly-around. The increased resolution provided by the 250 foot fly-around yielded the highest resolution photography to date of several module surfaces and supported detailed analyses. This fly-around photography is highlighted in Section 2.
  - The external configuration of the Mir Space Station for STS-86 was essentially the same as it was for STS-84. New additions to Mir include a sealant cover for the Spektr SP#1 mount currently stowed on the Docking Module, a centerline docking target replaced prior to undocking, and an unknown object attached to Spektr.
  - For the first time, video was obtained of the thermally-induced motion of a Mir solar array during the transitions between day and night. Video was acquired of the motion of Base Block SP#2 during three day-night and two night-day transitions. The magnitude of the measured motion ranged from 2 to 4 inches for the day-night transitions and 3.5 to 4 inches for the night-day transitions. The rates of motion were 0.02 to 0.04 inches/sec for the day-night transitions and 0.02 to 0.03 inches/sec for the night-day transitions. See Section 5.
  - An unknown substance is covering a purge port on the Kvant end dome. This port has appeared free of contaminants on previous mission photography. Section 3 provides an assessment of the condition of Kvant surfaces from the detailed photography acquired of the module on STS-86.
  - Peeled paint has been identified on Spektr handrails for the first time. In addition, a possible leak was observed in the corner of a Spektr radiator. For a description of these Spektr anomalies, see Section 3.
  - Photographs showed the capture and structural latches of the Mir Docking Module docking mechanism to be in proper position before docking and after separation. The laser retroreflectors and electrical connectors appeared to be in good physical condition, however the imagery was not of sufficient resolution to detect any discoloration which might exist. See Section 4.
  - Detailed, close-up photographs of the Mir Environmental Effects Payload (MEEP) experiments were taken during the EVA to retrieve the four experiment payloads. There was evidence of possible contamination of the Passive Optical Sample Assembly II (POSA II) in the form of numerous small brown spots visible on the outer casing and on areas of the experiment panel. The POSA I
-

- 
- photographs show what appears to be small white deposits on some of the circular, optical test specimens on the space-facing side of the payload. The Polished Plate Micrometeoroid and Debris (PPMD) and Orbital Debris Collector (ODC) payloads appeared to be in good condition. See Section 7.
- The position of the Kurs antenna attached to the Mir Docking Module was determined. This work was conducted in support of projected clearance calculations between the antenna and the Shuttle forward bulkhead for the planned STS-91 mission to be launched in May 1998. Statistical comparison of STS-84 and STS-86 results indicate the Kurs antenna moved between STS-84 and STS-86. Based on the STS-86 results, the projected clearance for STS-91 is 109.8 inches between the tip of the antenna and the Shuttle forward bulkhead. See Section 8.
  - The extensive number of small debris usually observed after Shuttle docking contact with Mir was not observed on STS-86. Several pieces of debris were noted during station-keeping. One piece of debris had an elongated, irregular-shaped appearance. Only two pieces of debris, other than those associated with the Spektr gas release event, were noted during the fly-around. None of the debris was observed to make contact with the Shuttle or Mir. See Section 6.
  - Video imagery was obtained of the Base Block SP#2 array motion in response to Orbiter and Mir thruster firings. The peak-to-peak displacement was measured to be approximately 0.10 inches. Error calculations place an uncertainty on this measurement of about  $\pm 0.10$  inches, and suggests that the peak-to-peak displacement of the motion is less than one-tenth of one inch. A description of the analyses and results are provided in Section 5.

Additional conclusions and recommendations are included as Section 10 of this Mission Report.

---

# Table of Contents

---

1. INTRODUCTION.....	1
2. MIR CONFIGURATION .....	2
3. MIR SURFACE ASSESSMENT .....	10
3.1 Spektr Damage Assessment.....	10
3.2 Surface Deposition/Discoloration and Damage .....	19
4. DOCKING MECHANISM ASSESSMENT.....	29
5. SOLAR ARRAY MOTION .....	31
5.1 Mir Structural Dynamics Experiment Solar Array Motion.....	31
5.2 Cooperative Solar Array.....	31
5.3 Thermally-Induced Motion of the Base Block Solar Array.....	32
6. DEBRIS DURING DOCKING OPERATIONS.....	36
7. MIR ENVIRONMENTAL EFFECTS PAYLOAD ASSESSMENT .....	39
8. POSITION OF THE KURS ANTENNA ATTACHED TO THE DOCKING MODULE.....	43
9. IMAGERY EVALUATION .....	47
9.1 Still Photography Review .....	47
9.2 Video Review.....	48
9.3 Crew Assessment .....	49
10. CONCLUSIONS AND RECOMMENDATIONS .....	51
10.1 Conclusions.....	51
10.2 Recommendations .....	52
11. REFERENCES .....	54
12. ACRONYMS & ABBREVIATIONS.....	55

## APPENDICES

Appendix A:	Preliminary Spektr SP#1 Geometric Deformation Analysis
Appendix B:	Assessment of Spektr Venting Test Imagery
Appendix C:	STS-86 Film Scenelist
Appendix D:	STS-86 Video Scenelist
Appendix E:	Sources for Report Imagery
Appendix F:	STS-86 Camera Layout

# Table of Contents

---

# List of Figures

---

Figure 2.1	+ZB Fly-around Overview of the Mir Space Station.....	3
Figure 2.2	-XB Backaway Overview of the Docking Module.....	4
Figure 2.3	+XB, +ZB Fly-around Overview of Spektr.....	5
Figure 2.4	+XB, +ZB Fly-around Overview of Priroda.....	6
Figure 2.5	-XB, +ZB Fly-around Overview of Kvant-2.....	7
Figure 2.6	+ZB Fly-around Overview of Kvant / Base Block .....	8
Figure 2.7	+XB, +ZB Fly-around Overview of Progress / Kvant.....	9
Figure 3.1	+XB, +ZB Overview of Spektr Module Damage .....	11
Figure 3.2	+XB, +ZB Spektr Radiator Damage.....	12
Figure 3.3	Close-up of +XB, +ZB Spektr Radiator Damage <b>Error! Bookmark not defined.</b>	
Figure 3.4	Cut Thermal Insulation on +ZB Surface of Spektr.....	14
Figure 3.5	+XB View of the Back Side of Spektr SP#1 and SP#3 Solar Array Damage.....	15
Figure 3.6	-XB View of the Front Side of Spektr SP#1 and SP#3 Solar Array Damage.....	16
Figure 3.7	-ZB Overview of Spektr SP#1 Damage.....	17
Figure 3.8	Close-up of Spektr SP#1 Sheared Support Beam.....	18
Figure 3.9	Close-up of Spektr SP#1 Sheared Support Beam.....	18
Figure 3.10	Close-up of Hole in Spektr SP#1 .....	19
Figure 3.11	Substance on end of Kvant End Dome Purge Port .....	20
Figure 3.12	Deposition on -ZB Kvant Radiator Surface .....	21
Figure 3.13	Deposition on +ZB Kvant Radiator Surface .....	22
Figure 3.14	Deposition on +ZB Kvant End Dome.....	23
Figure 3.15	Solar Cells Detaching from Kvant SP#1 .....	24
Figure 3.16	Possible Leak on Spektr Radiator .....	25
Figure 3.17	Chipped Paint on -XB, -ZB Handrails of Spektr.....	25
Figure 3.18	Deposition on +XB Surface of OPM Thermal Blanket .....	26
Figure 3.19	+ZB Discoloration and Damage on Base Block.....	27
Figure 3.20	-XB Deposition and Damage on Priroda .....	28
Figure 4.1	Photo of Docking Mechanism during Approach.....	29
Figure 4.2	Photo of Docking Mechanism during Backaway.....	30
Figure 5.1	Representative Video Frame of CSA during Undocking.....	32
Figure 5.2	Overview of Base Block SP#2 from Camera A.....	34
Figure 5.3	Representative Video Frames of Base Block SP#2 during a Night-to-Day Transition.....	33
Figure 6.1	Debris Observed Prior to Docking at GMT 270d:19h:17m:08s.....	36
Figure 6.2	Debris near ODS Prior to Docking at GMT 270d:19h:41m:35s .....	37
Figure 6.3	Debris after Undock at GMT 276d:17h:46m:53s .....	37
Figure 6.4	Rope-like Debris noted during Station-keeping at GMT 276d:18h:11m:28s .....	38
Figure 7.1	STS-86 Image of Mir with MEEP Experiments .....	39

## List of Figures

---

Figure 7.2	EVA Image of PPMD (left) and ODC (right).....	40
Figure 7.3	EVA Image of POSA II Showing Contamination.....	41
Figure 7.4	Images of the Same Section of POSA Taken on Four Separate Shuttle/Mir Missions.....	42
Figure 8.1	Kurs Antenna as seen from the Shuttle Flight Deck on STS-84.....	43
Figure 8.2	Kurs Antenna as seen from Payload Bay Camera A .....	44
Figure 8.3	Kurs Antenna as seen from Payload Bay Camera D .....	44

# List of Tables

---

Table 5-1	Analysis Results of Thermally-Induced Motion.....	35
Table 8-1	Coordinates of Kurs Antenna Tip .....	45

---

## 1. INTRODUCTION

As part of DTO-1118, approximately 1700 photographs and 54 hours of video of the Mir Space Station were acquired during the STS-86 mission.

The Image Science & Analysis Group (IS&AG) conducted several analysis tasks (based on user requirements) using the imagery data from STS-86. The purpose of the analysis tasks were to:

- Verify the configuration of the Mir complex.
- Assess the effect of micrometeoroid impacts and other visible damage on Mir surfaces.
- Compare the condition of Mir external surfaces to that seen on previous missions.
- Document the condition of the docking mechanism.
- Analyze solar array motion during Mir and Shuttle thruster firings in support of the Mir Structural Dynamics Experiment (MiSDE).
- Characterize debris seen during and after docking operations.
- Determine the position of the Kurs antenna attached to the Mir Docking Module in relation to the Shuttle for potential clearance issues on the subsequent STS-91 docking mission.
- Assess the quality of video and photographic data.

The following sections of this mission report describe the analyses, results, conclusions, and recommendations from STS-86.

---

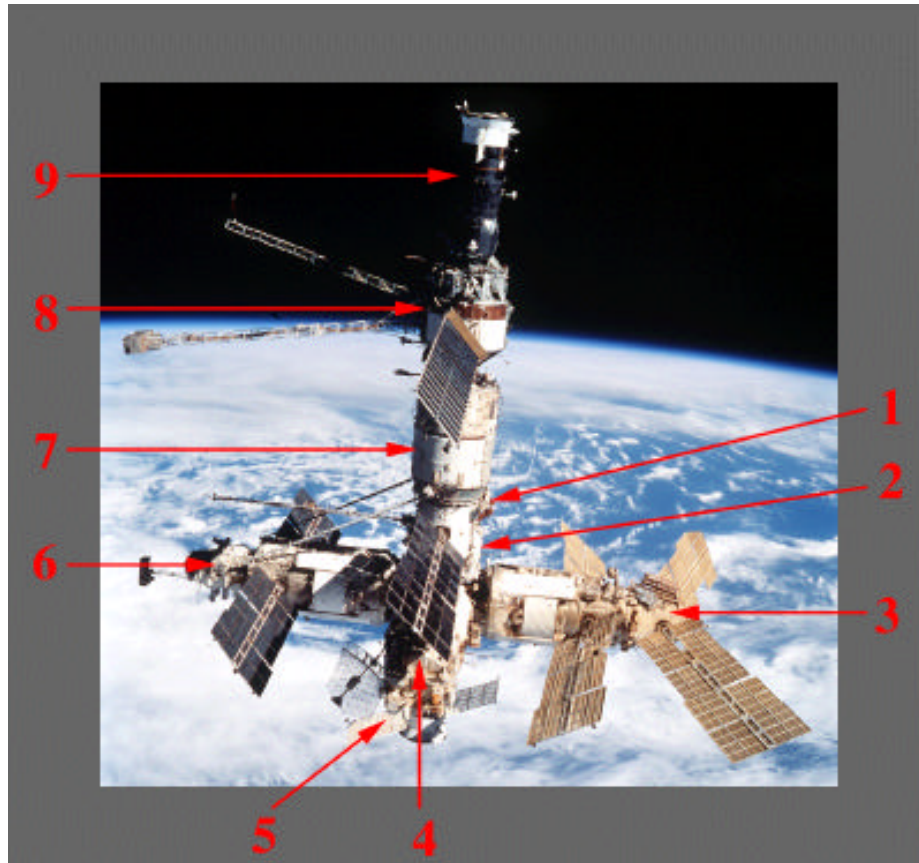
## 2. MIR CONFIGURATION

Information on the Mir configuration is important for proximity operations requiring visual navigation and for conducting simulations of structural loads on docked configurations. Configuration drawings of the Mir Space Station were compared to photography acquired during the STS-86 rendezvous and fly-around, and no significant differences were noted. The following paragraphs describe the configuration changes made both before and during the STS-86 mission.

The configuration of the Mir Space Station for STS-86 was essentially the same as it was for STS-84. The two new additions to Mir were an unidentified piece of hardware attached to the +XB, +ZB side of Spektr, and the sealant cover, for Spektr Solar Panel (SP) #1 mount, tethered to the Docking Module. The sealant cover was designed to seal-off leaks in the Spektr SP#1 attach if the array is removed.

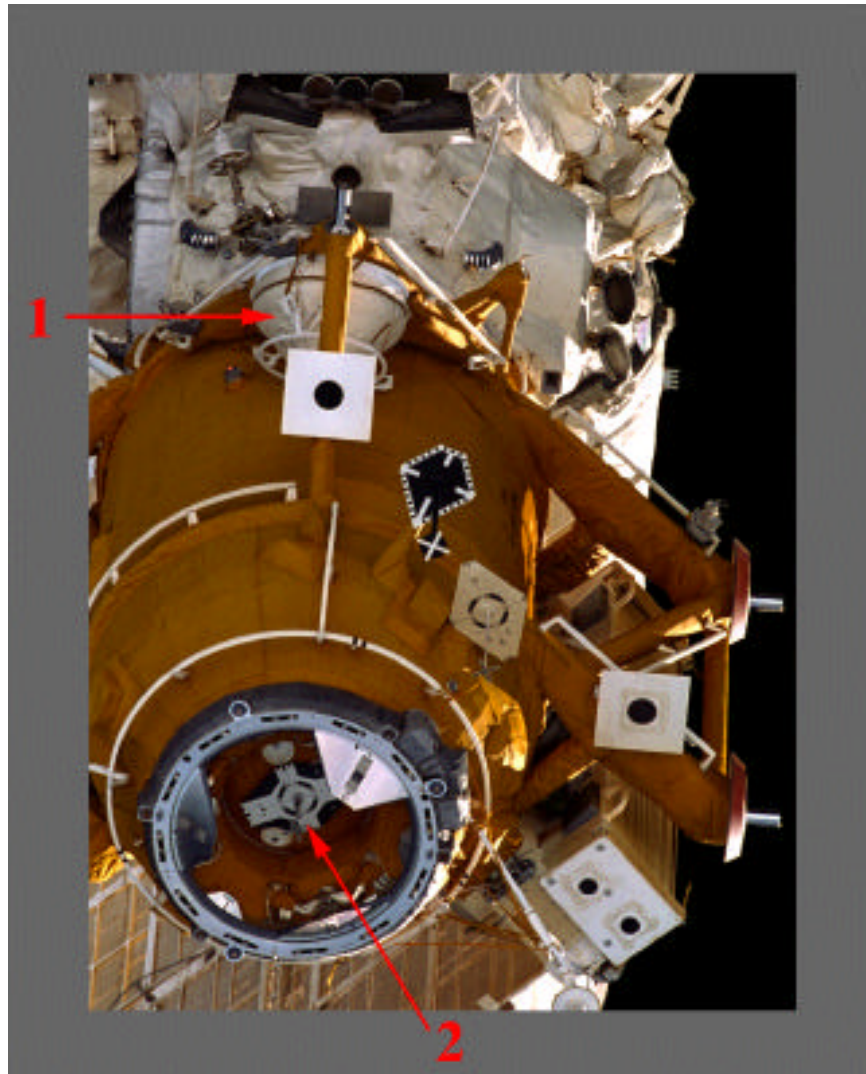
Two different experiments were removed from the Docking Module: The Optical Properties Monitor (OPM), which was removed prior to the STS-86 mission during an Extra Vehicular Activity (EVA), and the Mir Environmental Effects Payload (MEEP) experiment, which was removed during the STS-86 EVA.

Figure 2.1 provides an overview of the Mir modules in their STS-86 configuration. The backaway image of the Docking Module in Figure 2.2 identifies the Spektr SP#1 sealant cover, which was attached to the Docking Module during an EVA from the Shuttle, and the new Centerline Docking Target attached to the Docking Module hatch prior to undocking. The fly-around view in Figure 2.3 shows an unidentified feature on Spektr which has not been visible in previous mission photography. Figures 2.4 - 2.7 show fly-around photography which provides the highest resolution views to date of several modules.



**Figure 2.1 +ZB Fly-around Overview of the Mir Space Station**

- 1. Docking Module (obstructed)**
- 2. Kristall (obstructed)**
- 3. Spektr**
- 4. Priroda**
- 5. Soyuz**
- 6. Kvant-2**
- 7. Base Block**
- 8. Kvant**
- 9. Progress**



**Figure 2.2 -XB Backaway Overview of the Docking Module**

- 1. Sealant Cover for Spektr SP#1 Mount\***
- 2. New Centerline Docking Target**

\*New feature identified during this mission.



**Figure 2.3 +XB, +ZB Fly-around Overview of Spektr**

**1. Unknown\***

\*New feature identified for this mission.

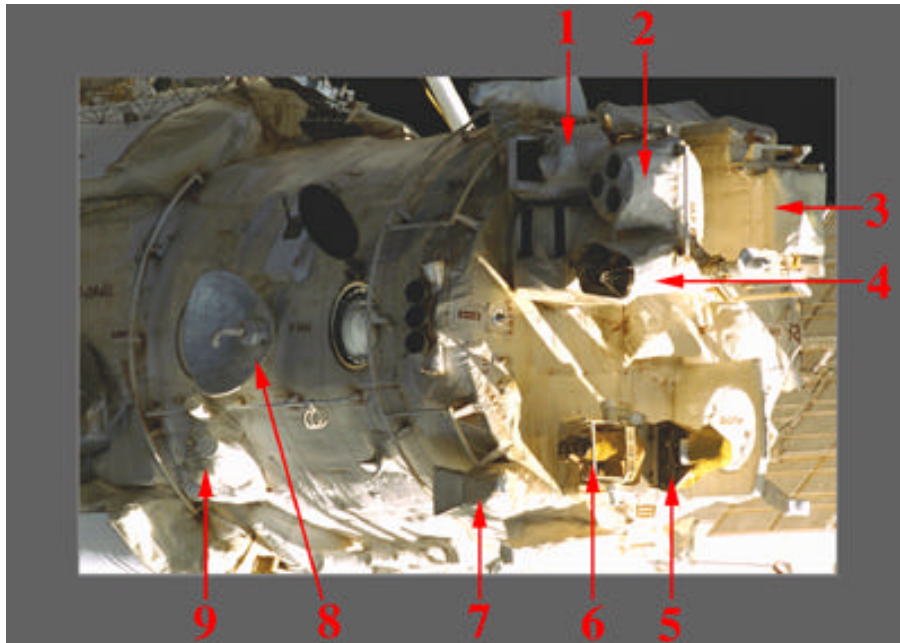


**Figure 2.4 +XB, +ZB Fly-around Overview of Priroda**

- 1. MSU-SK Multi-channel Scanning Device**
- 2. MSU-E Multi-channel Scanning Device**
- 3. Unknown\***
- 4. Unknown\***
- 5. Unknown\***
- 6. Unknown\***
- 7. IKAR-P**
- 8. Radiometer R-400**
- 9. Radiometer**

\*First identification of this feature.

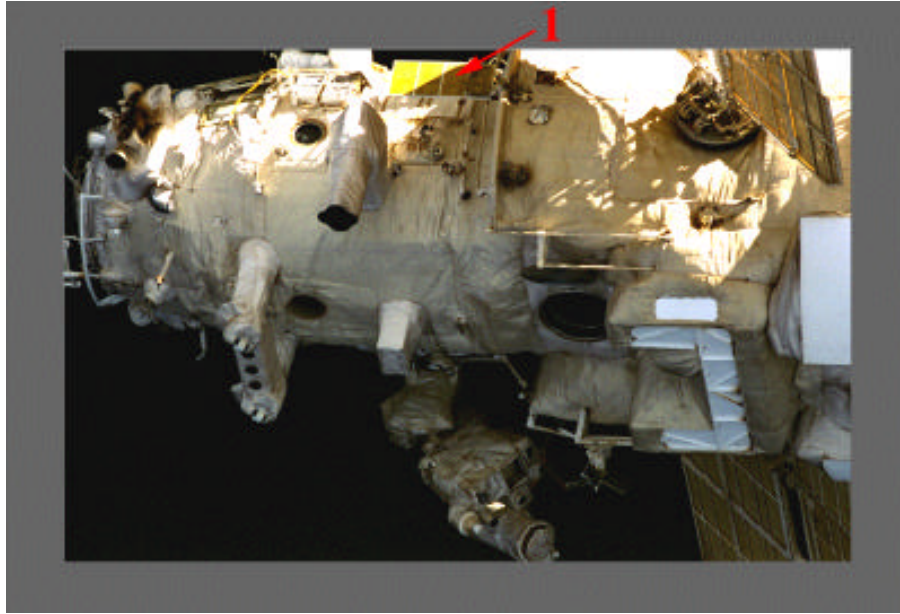


**Figure 2.5 -XB, +ZB Fly-around Overview of Kvant-2**

**1. Unknown\***

\*First identification of this feature.

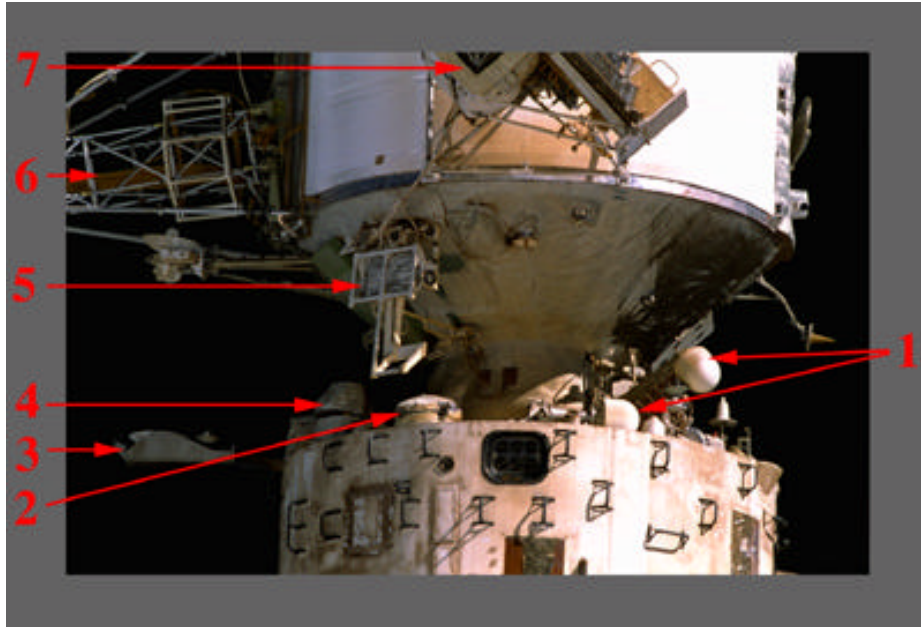


**Figure 2.6 +ZB Fly-around Overview of Kvant / Base Block**

- 1. “Igla” Antenna**
- 2. Unknown\***
- 3. “Igla” Antenna**
- 4. Unknown\***
- 5. Unknown\***
- 6. Sofora Truss**
- 7. Kvant SP#1**

\*First identification of this feature.

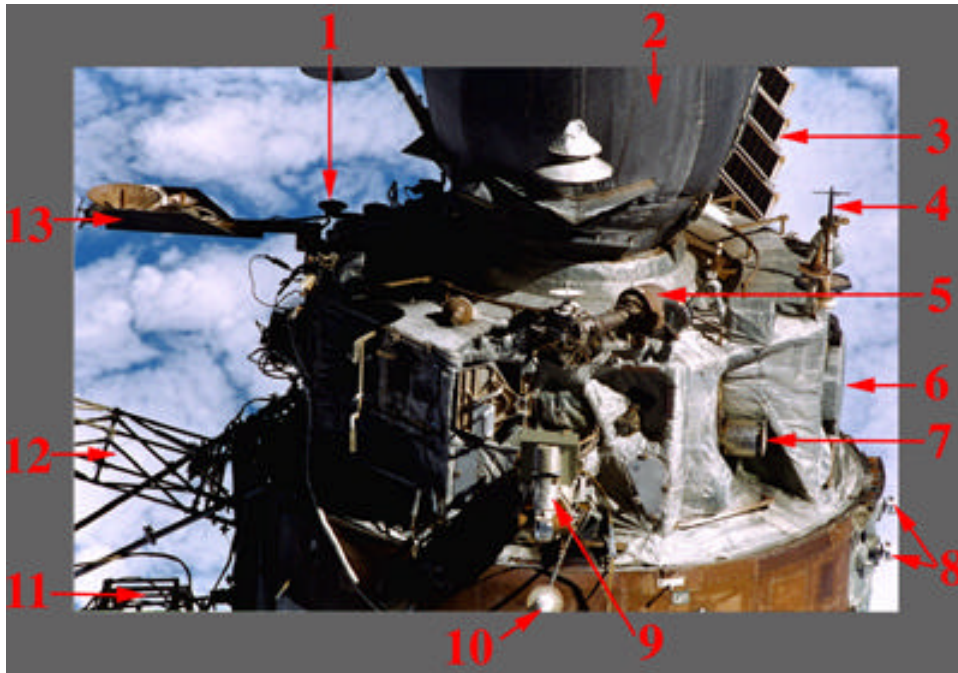


**Figure 2.7 +XB, +ZB Fly-around Overview of Progress / Kvant**

- 1. "Kurs" Antenna**
- 2. Progress**
- 3. Cooperative Solar Array (Kvant SP#2)**
- 4. Stand-off Target**
- 5. "Igla" Antenna**
- 6. "Glazar" Telescope**
- 7. Unknown**
- 8. Infrared Horizon Sensor**
- 9. Star Sensor**
- 10. "Kurs" Antenna**
- 11. Sofora Truss**
- 12. Ferma-3 Truss**
- 13. "Igla" Antenna**

---

### 3. MIR SURFACE ASSESSMENT

On June 25, 1997, during manual docking tests of the Progress resupply vehicle, the Progress collided with Spektr and caused damage to the Spektr module and solar arrays. During a Soyuz fly-around of Mir on August 15, 1997, Astronaut Michael Foale used a Hasselblad 70 mm camera with 100 mm and 250 mm lenses to take photographs of the damage. Foale's photography provides some unique views of the Spektr damage, especially the photographs which show the front surfaces of the damaged Spektr solar arrays. Imagery taken during the STS-86 fly-around of Mir provided the first opportunity to acquire detailed photography of the damaged Spektr module during a Shuttle-Mir mission. The Shuttle fly-around occurred at about the same distance as the Soyuz fly-around, which was approximately 240 feet. However, use of the 400 mm lens on the Nikon 35 mm camera during the Shuttle fly-around provided additional detail not seen in the Hasselblad photography from the Soyuz. Section 3.1 provides an assessment of this damage.

An assessment of the condition of the exterior surfaces of Mir was made from STS-86 DTO-1118 survey imagery, and except for areas of Spektr, the extent of damage/deterioration seen on Mir surfaces does not appear to have significantly changed since STS-84. In addition to the fly-around imagery, photography and video of Mir obtained during approach, while the Shuttle was docked to Mir, and during backaway was used to perform an overall Mir surface assessment. Section 3.2 describes areas of damage and discolorations, which are unrelated to the Progress incident.

#### 3.1 Spektr Damage Assessment

Imagery analysis indicates that the exterior damage to Mir from the Progress collision is limited to the appendages and surfaces of the Spektr module. Damage to Spektr's SP #1 includes: a bent corner on the first sub-panel of the array closest to the attach, a bend in an upper corner of the second sub-panel, a sheared center support beam which is also separated, a center support beam which appears sheared but not separated, a hole through the third sub-panel, and a broken and bent support in the seventh sub-panel. In addition, the axis of the array has been deflected approximately 8 degrees in the -YB direction and is no longer aligned with SP#2 on the opposite side of the module. The only other Spektr solar array which appears to have been damaged in the collision is SP#3. A support beam on the third sub-panel of SP#3 is bent, and there is a surface scrape mark on the backside of the array adjacent to this beam.

Damage to the surface of the module appears to be limited to the +XB, +ZB radiator, which is significantly distorted (dented, bent, and creased). In addition, the area of thermal insulation, which was cut along an edge of the +XB, +ZB radiator during an EVA, is visible in photography.

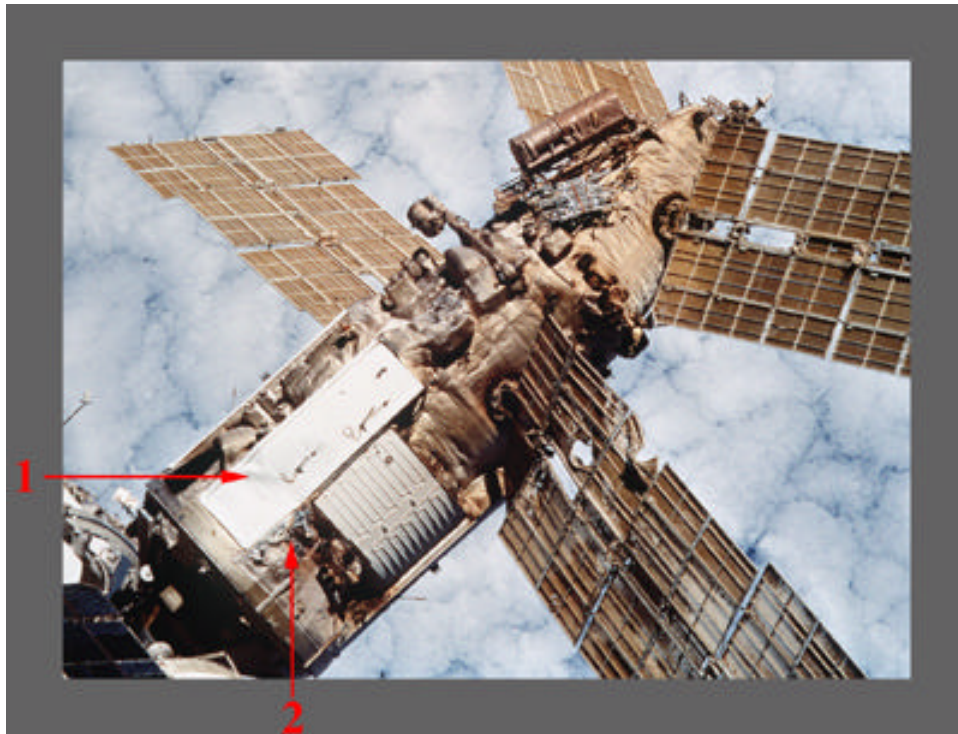
IS&AG has performed two in depth analyses of the Spektr damage. They are included as Appendices A and B of this report and are the "Preliminary Spektr SP#1 Geometric Deformation Analysis" and the "Assessment of Spektr Venting Test Imagery".

---

The following paragraphs describe the damage to Spektr identified from the STS-86 and Soyuz imagery. Overview images are shown, followed by detailed imagery and analyses.

### Module Damage

Figure 3.1 is an overview photograph which shows the damage sustained to the surface of the Spektr module. This photograph provides a face-on view of the damage to the +XB, +ZB radiator [1]. The photograph also shows the thermal insulation [2] that was cut so that a camera could be inserted under the radiator in an attempt to find the source of the leak in the module.



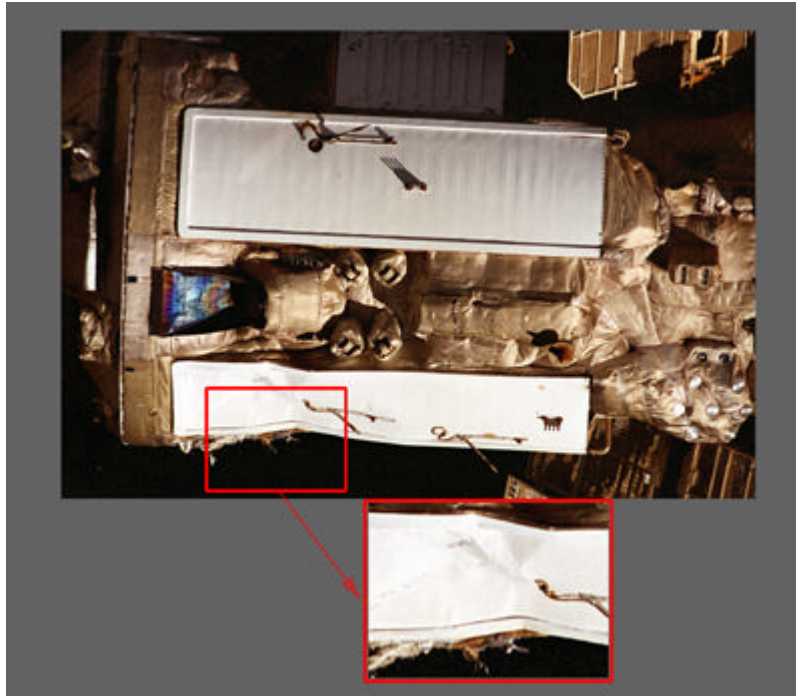
**Figure 3.1 +XB, +ZB Overview of Spektr Module Damage**

Figure 3.2 is a more detailed photograph of the +XB, +ZB radiator on Spektr. The bend in the radiator covers the entire width of the radiator and approximately one-third of the length of the radiator from where the module connects to the Station node. The approximate depth of the bend along an outer edge was estimated from oblique photography to be approximately 10 cm. This measurement is an estimate of the amount the radiator was displaced by the Progress impact.

Figure 3.3 is a close-up photograph of the bend in the +XB, +ZB radiator on Spektr. This photograph, taken from a Base Block window, provides detail on the texture of the bend in the surface of the radiator. Arrows in the figure are used to indicate the locations where the Progress likely contacted the surface of the radiator. One of the areas where

---

Progress contacted the surface appears to have a wide scrape [1]. There also appears to be a long, narrow shadow cast by a possible piece of thermal insulation [2]. There are several pieces of apparent thermal insulation which are probably residues of the EVA thermal insulation cutting activity performed to look for leaks in the surface of Spektr under the bent radiator. The results of this EVA activity are highlighted in Figure 3.4.



**Figure 3.2 +XB, +ZB Spektr Radiator Damage**

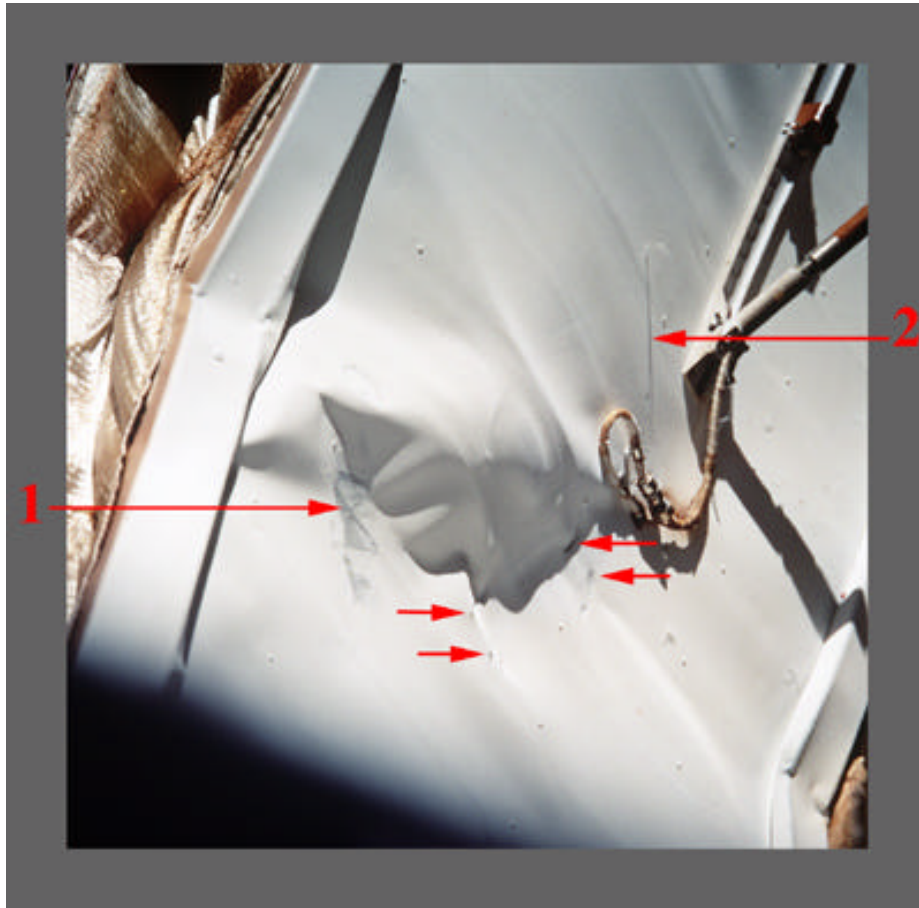
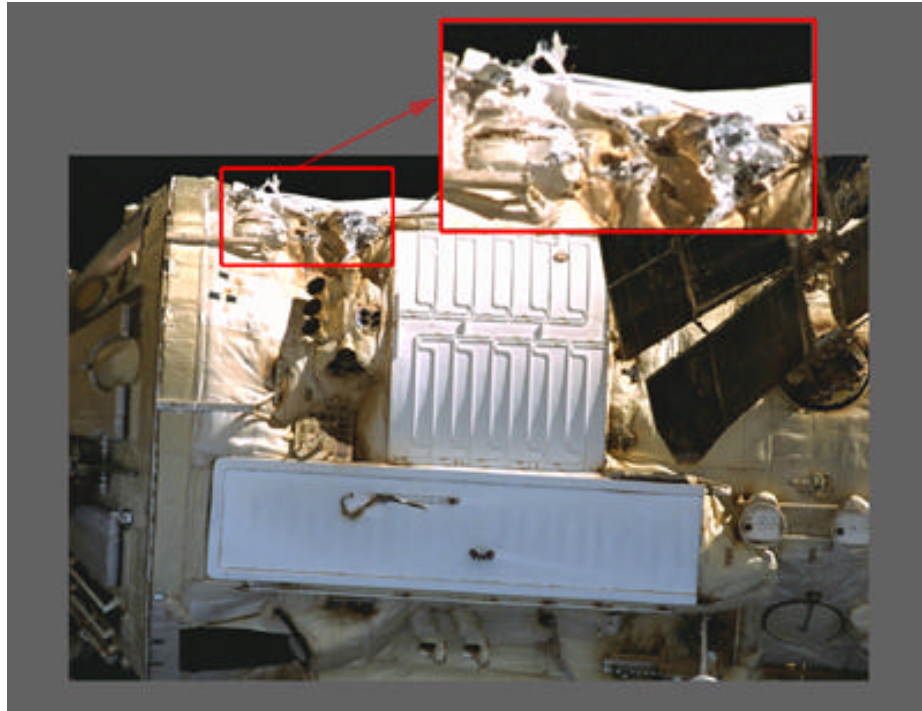


Figure 3.3 Close-up of +XB, +ZB Spektr Radiator Damage

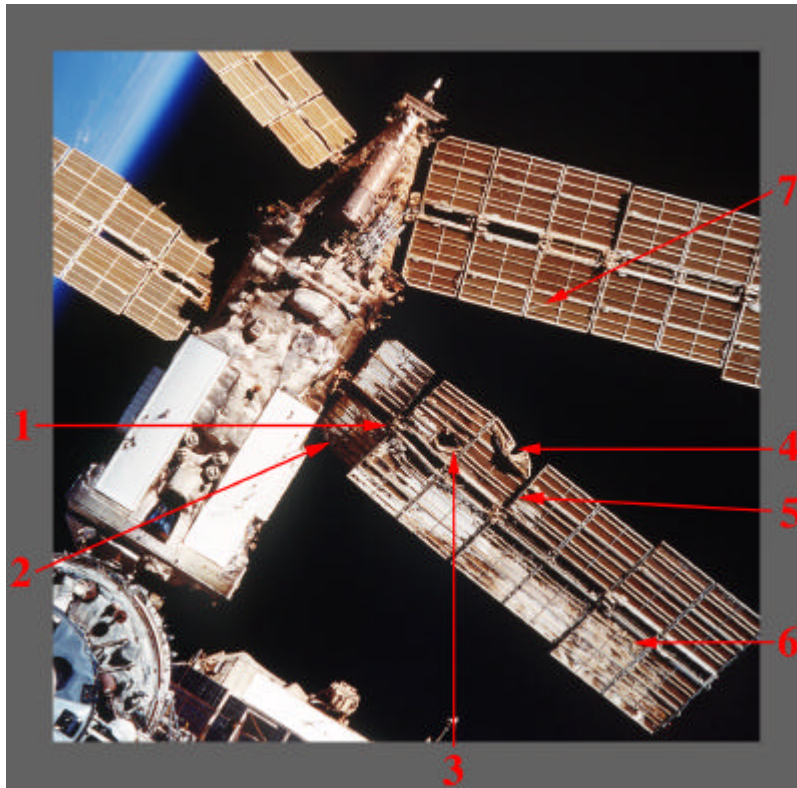


**Figure 3.4 Cut Thermal Insulation on +ZB Surface of Spektr**

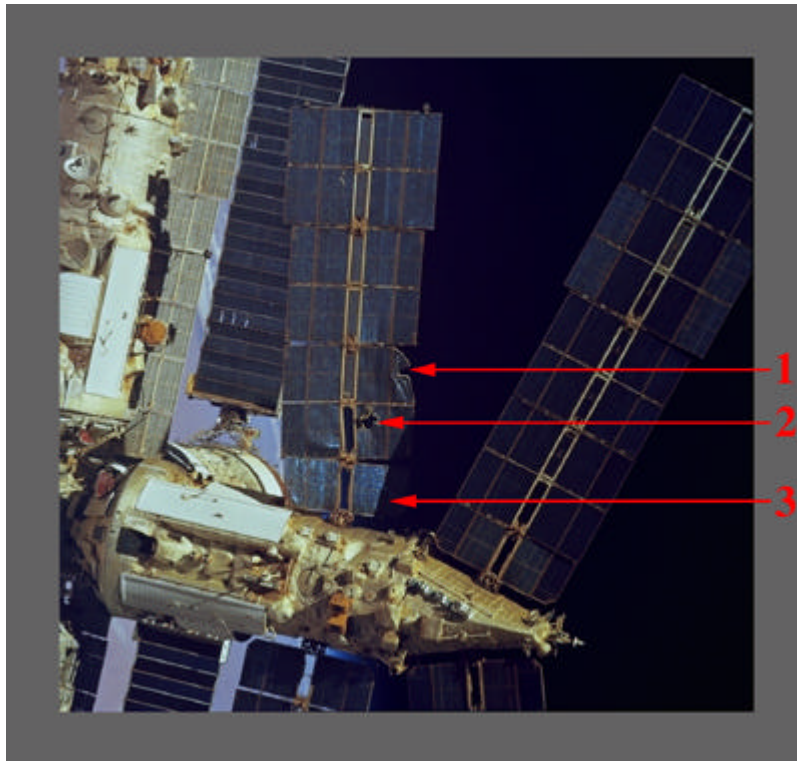
### Solar Array Damage

Figure 3.5 is an overview photograph which shows the back-side of all solar array surfaces which were damaged during the Progress collision. Damaged areas of SP#1 are indicated by Items 1-6, and damage to SP#3 is indicated by Item 7. One of the two separate support beams which make up SP#1's central support structure has sheared next to what appears to be a weld joint [1]. The other beam also appears to have sheared, but the sheared ends appear to remain in contact with each other. Dividing each array into seven major sub-panels, these sheared center beams are located just above the break between the first and second sub-panels from the array's attach point on Spektr. The first sub-panel has a bent corner [2], and there is a large hole through the second sub-panel measured to be 0.25 m<sup>2</sup> in area [3]. An upper corner of the third sub-panel is severely bent [4], the lower edge of the fourth sub-panel is bent [5], and one of the supports in the seventh is broken and bent out of the frame [6]. On SP#3, a support in the third sub-panel is bent, and there appears to be a scrape mark on the back side of the solar panel adjacent to this support [7].

Figure 3.6 shows a photograph taken during the fly-around of Mir by Soyuz. This view shows the front surface of the Spektr arrays. The severe bend in the upper corner of the third sub-panel [1] and the large hole through the second sub-panel [2] can be seen in this photograph. Note that the edge of SP#3 is shadowing the lower corner of SP#1 [3].



**Figure 3.5 +XB View of the Back Side of Spektr SP#1 and SP#3 Solar Array Damage**



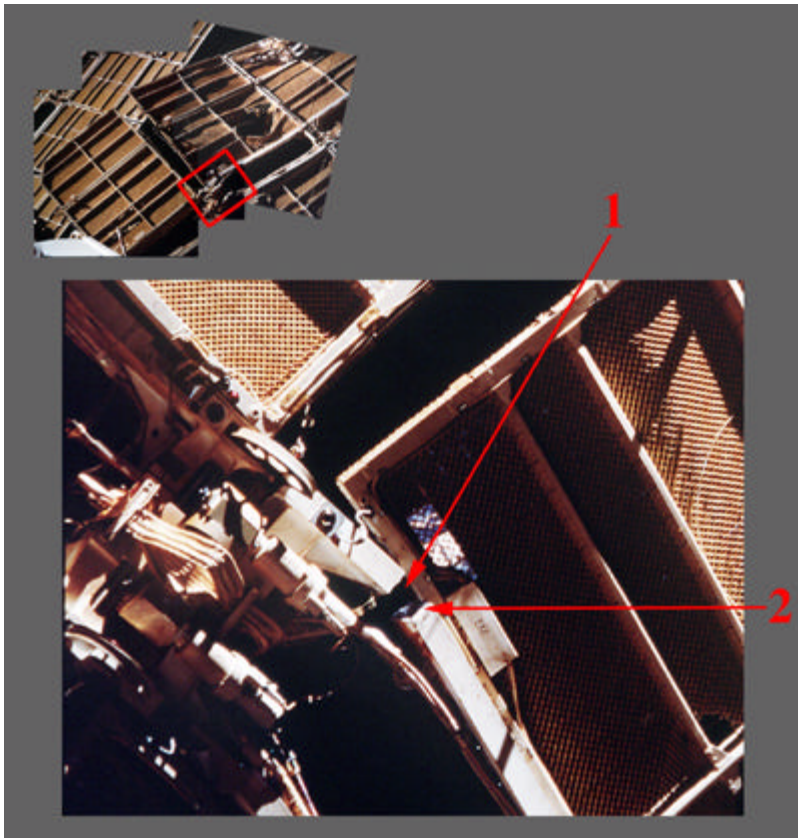
**Figure 3.6 -XB View of the Front Side of Spektr SP#1 and SP#3  
Solar Array Damage**

Figure 3.7 is a photograph of Spektr SP#1, taken from the -ZB perspective, which shows the back-side of the array. The highlighted region at the top of the figure provides a magnified view of an upper corner of the third sub-panel, which is severely bent [1]. The lower edge of the fourth sub-panel is bent [2]. The magnified view at the bottom of the figure shows the damage on the seventh and eighth sub-panels. One of the supports in the seventh sub-panel is broken and bent out of the frame [3]. A support wire running across the back of the eighth sub-panel is loose, suggesting it snapped in the collision [4].



**Figure 3.7 -ZB Overview of Spektr SP#1 Damage**

Figure 3.8 is a close-up photograph of the damage to SP#1's central support structure. One of the two beams has sheared and separated completely [1]. The beam has a clean break along what appears to be a weld joint [2]. The beam along the other side of the central support structure is in shadow in this photograph. Figure 3.9 shows the damage to the support beam adjacent to the beam described in Figure 3.8. In the photograph on the left, the upper section of the beam [1] above the sheared region appears to be pushed back and to the left of the lower section of the beam [2] adjacent to the array attach. The image on the right provides a view of the other side of the array and supports the description of the damage from the image on the left. As expected, the upper portion of the beam [3] appears to be to the left and extending further toward the image plane than the lower portion of the beam [4]. Based on these two observations, the upper and lower sections of the beam appear to be in contact even though the beam appears sheared.



**Figure 3.8 Close-up of Spektr SP#1 Sheared Support Beam**

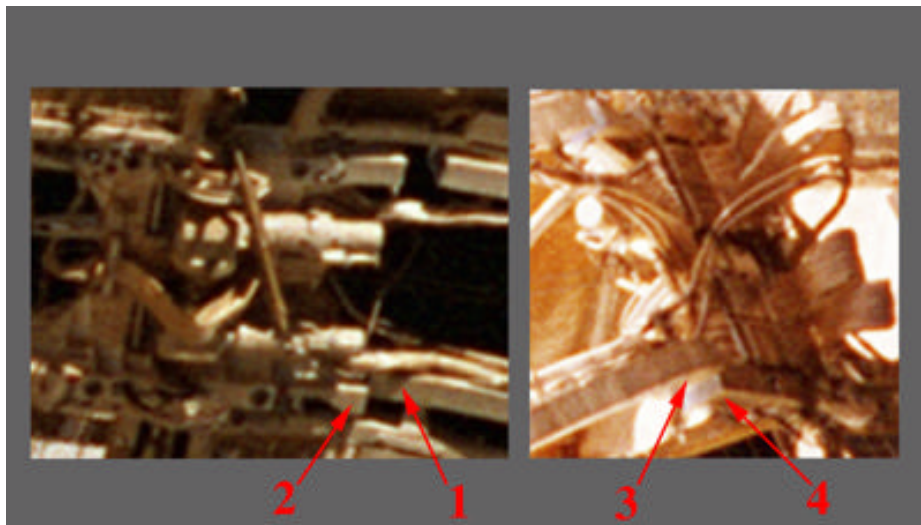


**Figure 3.9 Close-up of Spektr SP#1 Sheared Support Beam**

---

Figure 3.10 is a close-up photograph of the hole in SP#1's second sub-panel [1]. The hole area was measured to be approximately 0.25 m<sup>2</sup>. A support wire [2] running across the back of the sub-panel is also broken. There appears to be support wires running diagonally across the back of all sub-panels.

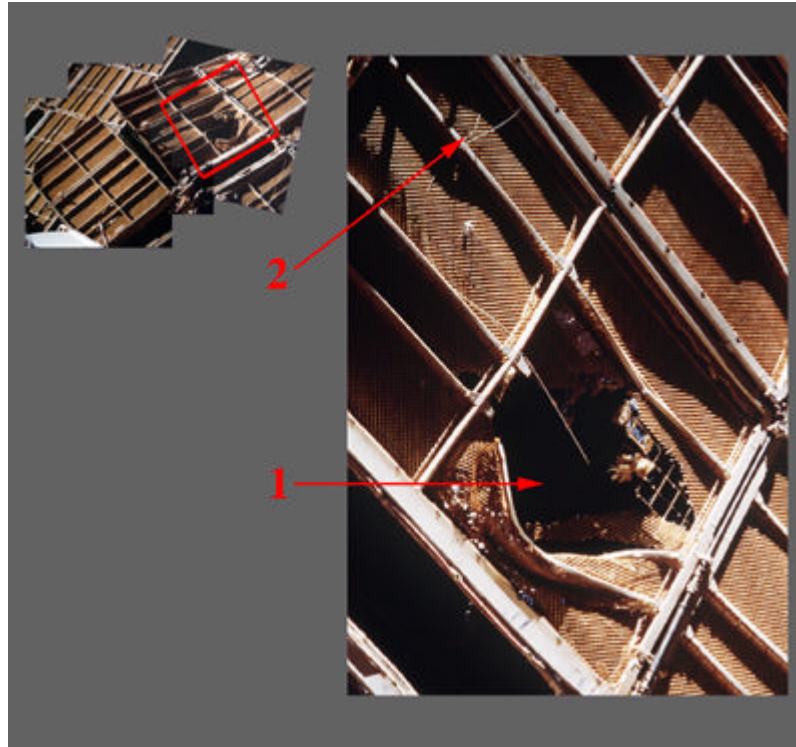


**Figure 3.10 Close-up of Hole in Spektr SP#1**

### **3.2 Surface Deposition/Discoloration and Damage**

Imagery taken of Mir starting with STS-63 (February 1995) has revealed deposition/discoloration on all Mir modules and has been documented in all previous mission reports. The deposition/discoloration portion of this report focuses on the surfaces of Mir which were photographed in detail during the STS-86 fly-around. New details of deposition/discoloration are observed in photographs of Kvant and the Base Block. This new detail provides the ability to compare surfaces of these modules not visible during the docked phase. New photography of the Kvant SP#1 shows that additional strips of solar cells have begun to lift off the surface of the array since the last detailed photography of Kvant SP#1 was taken on STS-79. Damage to a micrometeoroid sensor on the Base Block and a possible leak on Spektr are also discussed. In addition, mission photography

---

reveals a substance on the end of a Kvant end dome purge port. This port has appeared free of contaminants on previous mission photography.

Kvant Purge Port

Figure 3.11 is a comparison of photographs between STS-84 and STS-86 of the purge ports located on the Kvant end dome adjacent to the Base Block. The photograph on the left shows one of the purge ports [1] to be free of any contaminants. This port has appeared free of contaminants on previous missions where it was visible (STS-79 and STS-81). The photograph on the right reveals a white substance which covers this same purge port [2], and there appears to be spots of a similar substance on some surfaces adjacent to the port.

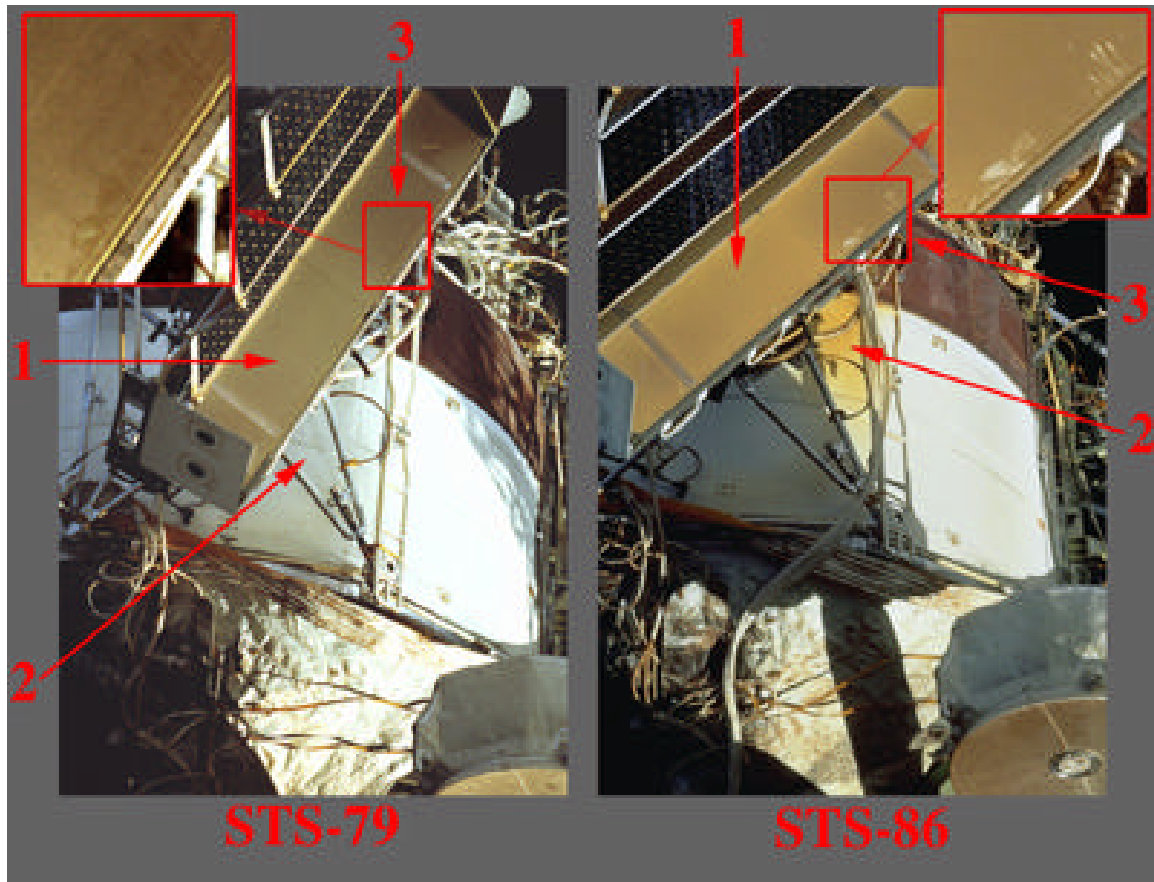


**Figure 3.11 Substance on end of Kvant End Dome Purge Port**

Kvant -ZB Array Attach Point

Figure 3.12 is a comparison of photographs between STS-79 and STS-86 which show the attach region of the CSA. The CSA was deployed on the Kvant -ZB axis on May 25, 1996. The photograph on the left was taken in late September 1996 (during STS-79). The CSA carrier [1] and the Kvant radiator surface [2] appear to be free of discoloration in this photograph. However, the photograph on the right, taken 16 months later on STS-86, shows apparent discoloration on both the CSA carrier [1] and Kvant radiator surface [2] which appears brown in color, and may be caused by a contaminant deposited on the

surface. There also appears to be a preferential pattern to this deposition on the radiator surface. The heaviest deposition appears to be occurring in the +XB, +YB direction away from the CSA attach point. However, the extent of the pattern cannot be identified since the array is obstructing much of the view of the surface of the Kvant radiator. There are some thin lines of brown discoloration on the CSA carrier in the photograph taken during STS-79 [3]. These same lines appear white in the photograph taken during STS-86 [3]. Except for this feature [3], the rest of the carrier is darker and appears to have additional deposition.



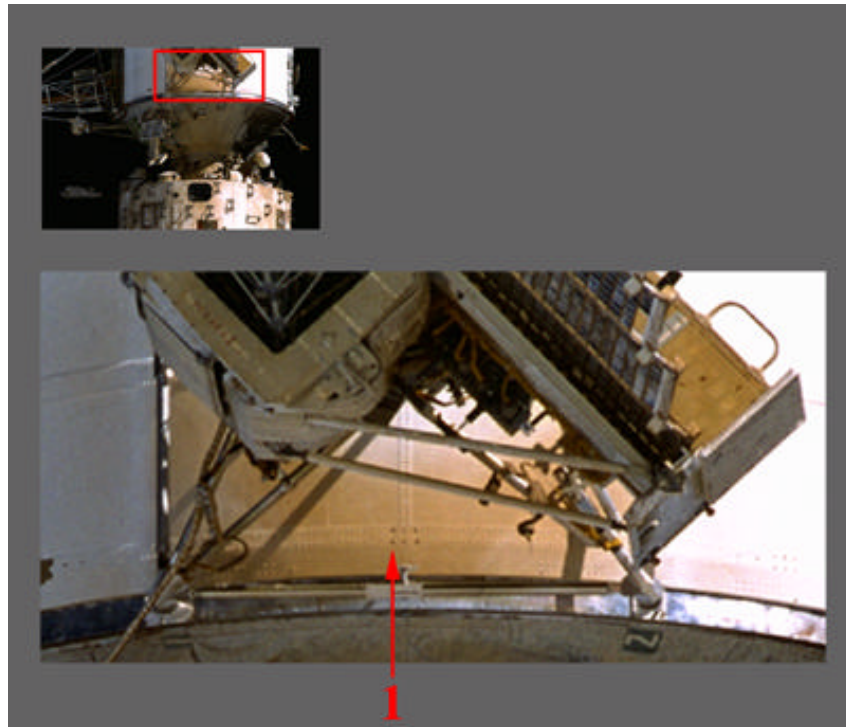
**Figure 3.12 Deposition on -ZB Kvant Radiator Surface**

Figure 3.13 is the highest resolution photograph to date of the +ZB SP#1 attach point on Kvant. The discoloration [1] seen on the Kvant radiator surface below the attach point appears similar to the discoloration seen in Figure 3.12. Like Figure 3.12 of the -ZB radiator surface, there also appears to be a preferential pattern to the deposition on the +ZB radiator surface. The heaviest deposition on this side appears to be occurring in the -XB, +YB direction away from the SP#1 attach point. Although the array is obscuring the view of the Kvant radiator surface, other photographs verify this preferential pattern of deposition as well. This deposition is not occurring in the same direction from the array attach as the deposition on the other side of the module.

#### Kvant End Dome

---

Figure 3.14 is the highest resolution photograph to date of the +ZB side of the Kvant end dome. There is dark deposition [1] covering approximately 25 percent of the +ZB side of the end dome facing the +YB direction, while the rest of the end dome appears to have little deposition or discoloration. There is a similar dark deposition covering approximately 50 percent of the -ZB side of the end dome facing the +YB direction. The deposition on each of these sides appears to be caused by the same source, due to the similar appearances and close proximity of the depositions around the circumference of the end dome. Approximately 40 percent of the periphery of the end dome shows deposition.



**Figure 3.13 Deposition on +ZB Kvant Radiator Surface**

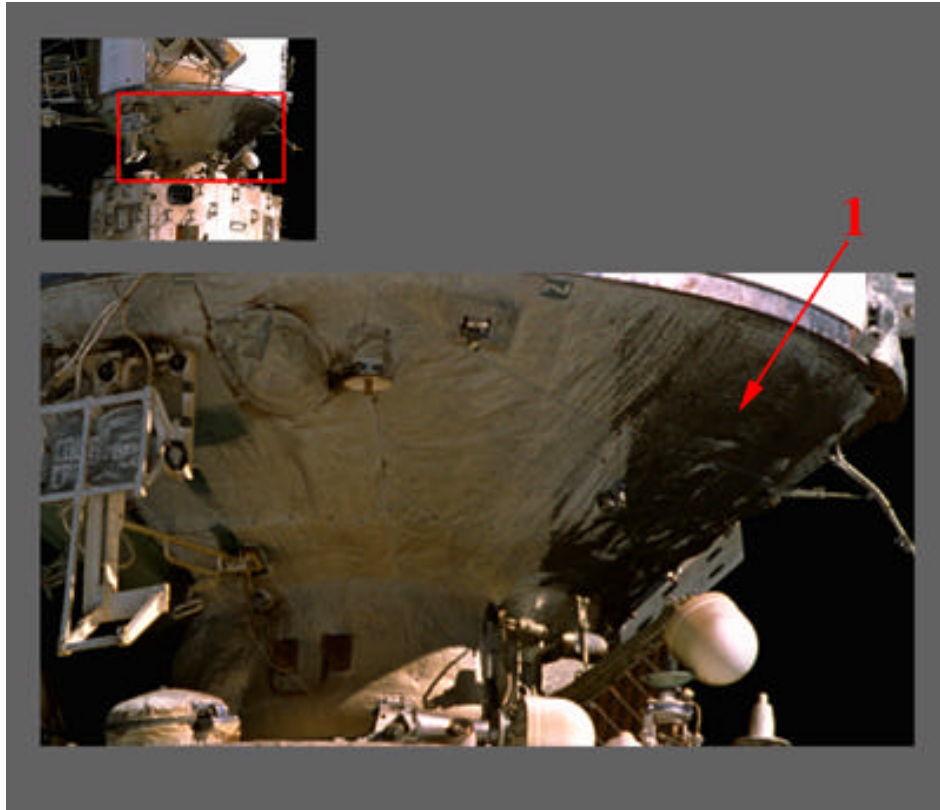


**Figure 3.14 Deposition on +ZB Kvant End Dome**

Kvant SP#1

Figure 3.15 is a comparison of photographs taken on STS-79 and STS-86 which both show strips of solar cells detaching from the wire frame of Kvant SP#1. The photograph on the left shows two strips of solar cells lifted off the support frame of the array [1], while the photograph on the right shows that a third strip of solar cells, in the middle of the first two, is also lifted off the support frame [2]. Other strips of solar cells were first observed lifted off the support frame of the array on STS-71, and this type of anomaly has not been seen on other Mir arrays.

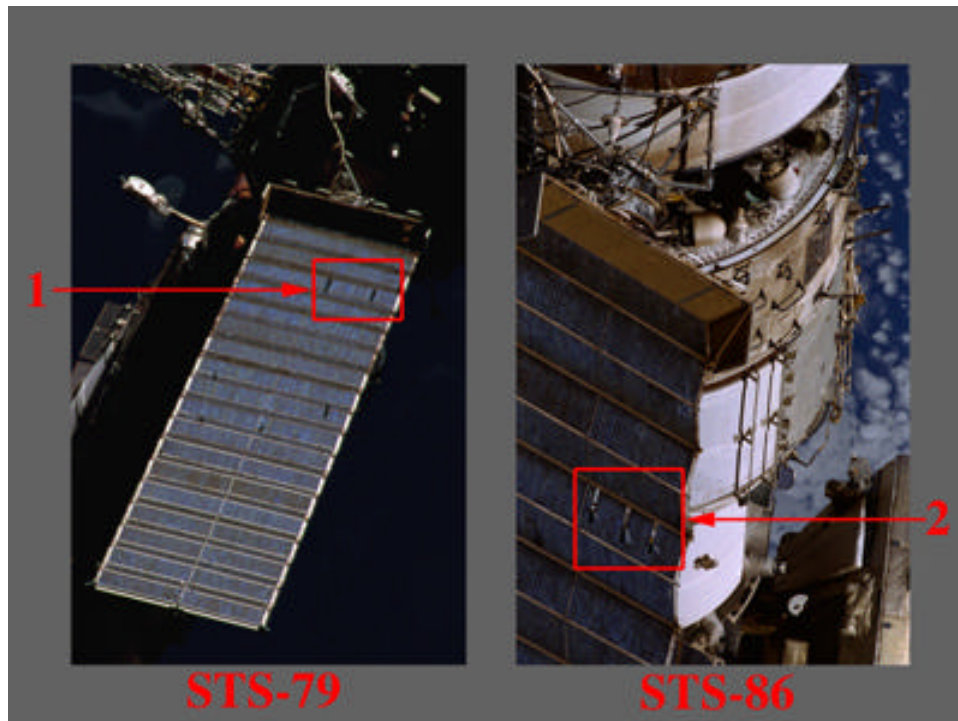
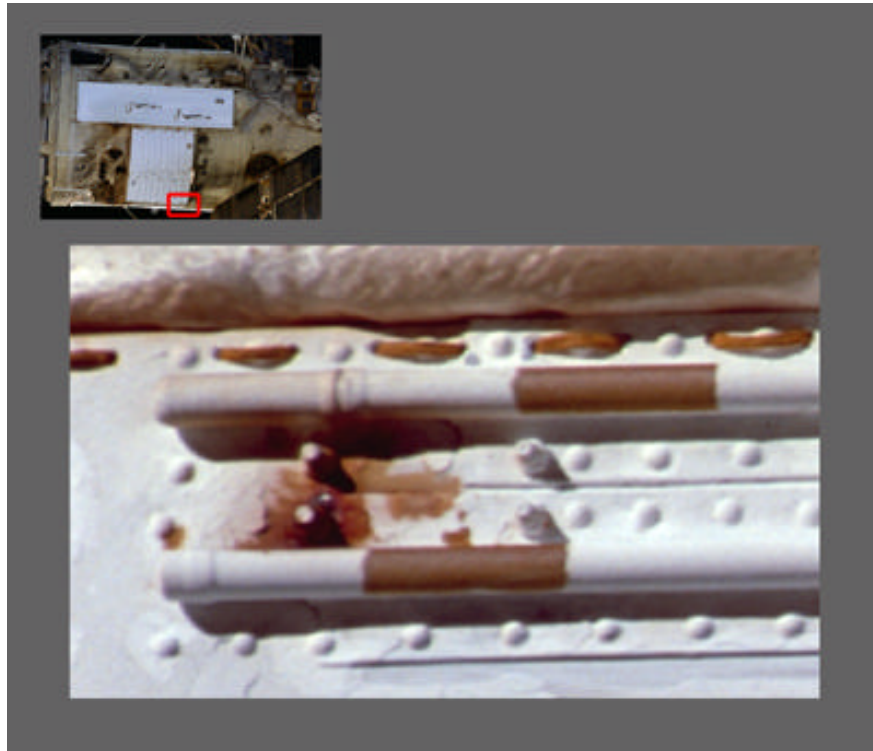


**Figure 3.15 Solar Cells Detaching from Kvant SP#1**

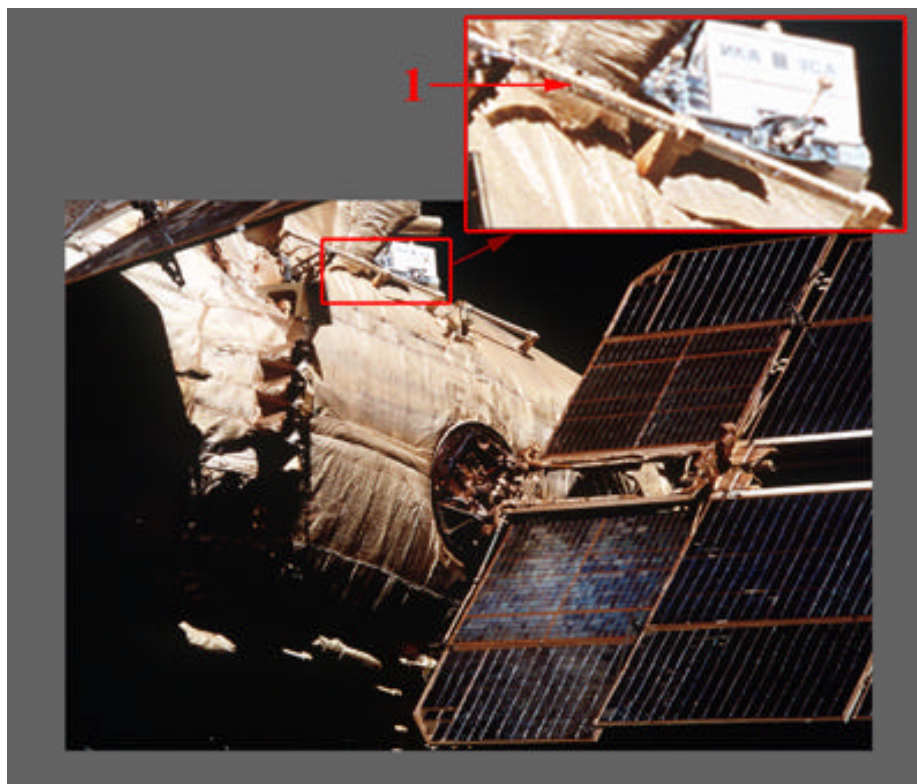
### Spektr

Figure 3.16 is the highest resolution photograph to date of a possible leak around bolts and rivets on the +XB, -YB corner of the Spektr radiator. A possible leak was previously identified on the +YB side of the radiator. (Reference 6.) This leak on the +XB, -YB corner was visible on all missions where this radiator was facing the Shuttle, however, the lower resolution of previous mission imagery does not allow for a comparison of leak size to determine if the leak has grown. From this image, the size of the stain left by the leak was determined to be approximately 9 cm<sup>2</sup>. The dark areas on top of the tubing are hold-down brackets and are not part of the leak.

Figure 3.17 is the first photograph identified which shows chipped paint on Spektr handrails [1]. Spektr docked with Mir in June, 1995, therefore this paint has begun to chip or peel within the first 28 months of the module's deployment.



**Figure 3.16 Possible Leak on Spektr Radiator**



**Figure 3.17 Chipped Paint on -XB, -ZB Handrails of Spektr**

---

## Optical Properties Monitor on the Docking Module

Figure 3.18 is a comparison of photographs of the OPM between STS-84 and STS-86. The OPM was deployed on the Docking Module during an EVA on April 29, 1997. The image on the left, taken in May 1997 during STS-84, reveals a highly preferential pattern of discoloration on a thermal blanket covering the end of the OPM facing the +XB direction. The image on the right, taken on STS-86 approximately 4 months later, indicates that the discoloration is now more uniform across the surface of the thermal blanket. However, there are areas to the left of the handrail attach points that appear to be receiving little deposition [1]. These handrail supports protruding from the surface appear to block the deposition which is striking the rest of the thermal blanket, creating a “shadow” of the supports to the left of the actual supports. In addition, there is a small flap of thermal blanket, stitched back along a seam to the right of the lowest handrail attach point, which appears to be receiving less deposition than the thermal blanket adjacent to it [2]. This flap may be shielded by areas of thermal blanket adjacent to it which protrude higher off the surface of the experiment carrier. In general, the discoloration on the +ZB half of the experiment appears darker brown in color than the -ZB half [3 & 4 respectively].

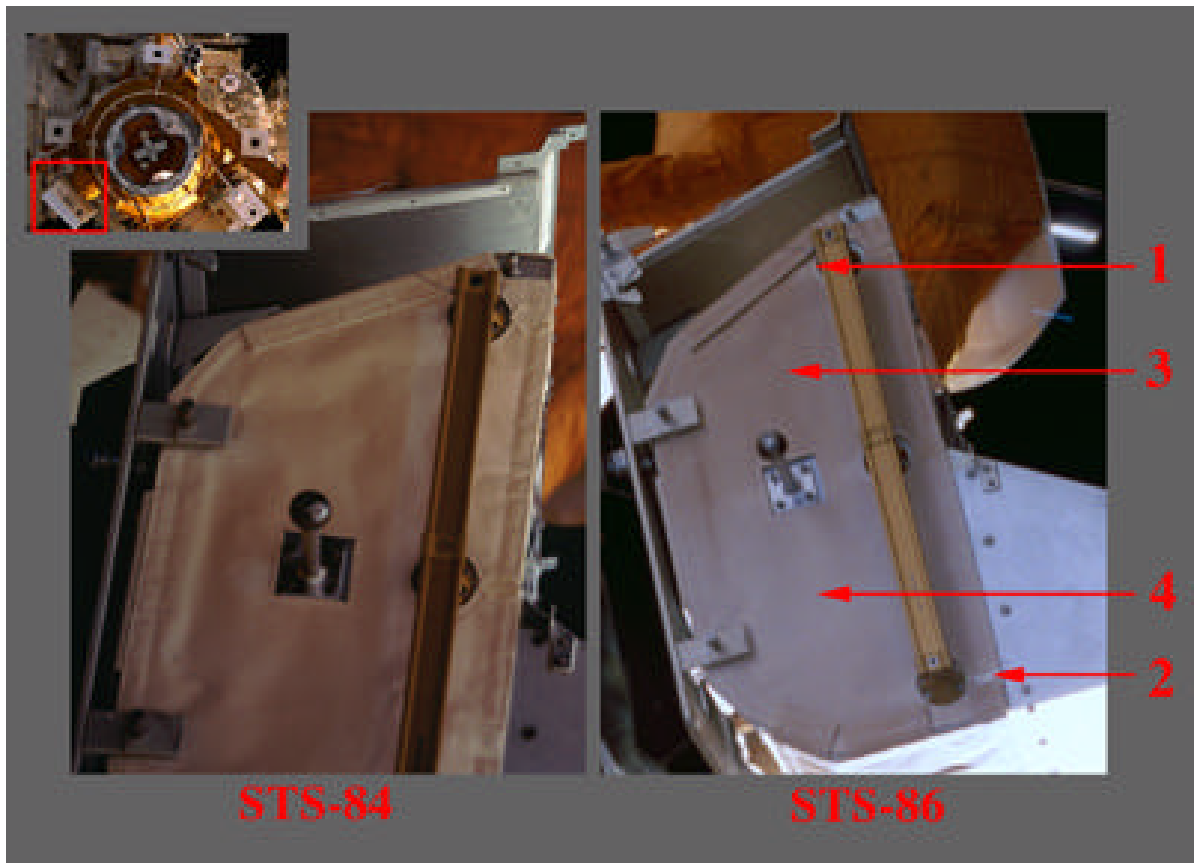


**Figure 3.18 Deposition on +XB Surface of OPM Thermal Blanket**

---

## Base Block

Figure 3.19 is the highest resolution photograph to date of the +ZB side of the Base Block. This image verifies that the pattern of general discoloration and damage seen on the surface of the Base Block is uniform around the circumference of the module. There are areas of non-preferential discoloration [1], and areas of preferential discoloration [2] which appear to follow along the seams of the module surface. Two of the four micrometeoroid impact sensors mounted around the circumference of the Base Block can be seen in this photograph. Damage on one of these sensors [3] was reported previously in the STS-63 report. Looking at the enlarged inset of the other sensor, this photograph provides new details on the condition of the sensor. The top layer of one of the outer panels appears to be missing completely [4], leaving the possible middle layer which appears red in color. Approximately 25% of the top layer of the other outer panel [5] and 50% of the inner panel [6] remains intact. Approximately 65% of the middle layer and 10% of the bottom layer of the outer panel [5] is visible, while approximately 20% of the middle layer and 30% of the bottom layer of the inner panel [6] is visible. Compared to the damage on the other sensor [3] which was reported previously, the damage on the highlighted sensor appears more uniform.

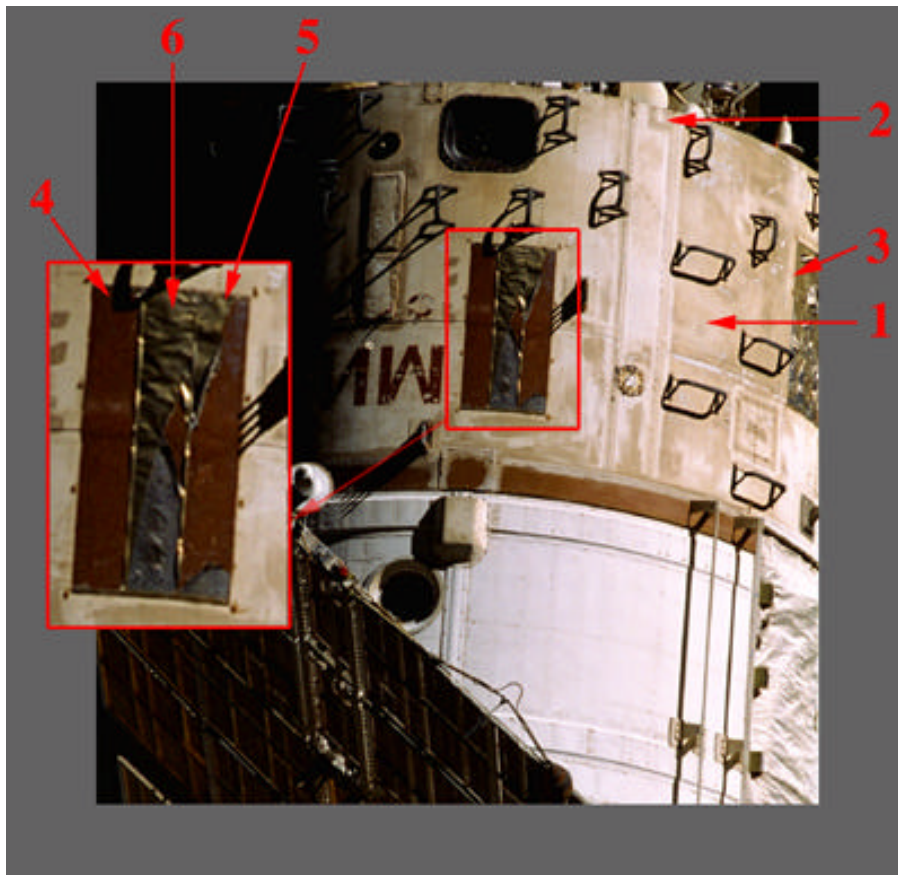


**Figure 3.19 +ZB Discoloration and Damage on Base Block**

---

## Priroda

Figure 3.20 is the highest resolution photograph to date of the -XB side of Priroda. Deposition [1] is visible on the thermal insulation directly below three attitude control thruster nozzles. This deposition is similar to deposition previously noted around thruster nozzles on other modules such as Kvant-2 and Spektr. There are also a couple of anomalies on the surfaces of the Delta-2P Radiometer [2]. The radiometer dish, which is extended perpendicular to the surface of Priroda, has some discoloration which appears preferential-oriented. Two regions of the dish do not appear as discolored as the rest of the dish. If the discoloration is caused by the deposition of some contaminant on the dish, objects surrounding it may be shadowing areas so that they receive less deposition. The radiometer dish, which is mounted flat against Priroda, appears to have some surface damage. The texture pattern just off the center of the dish suggests that the outer covering of the dish may be peeling off the surface [3].

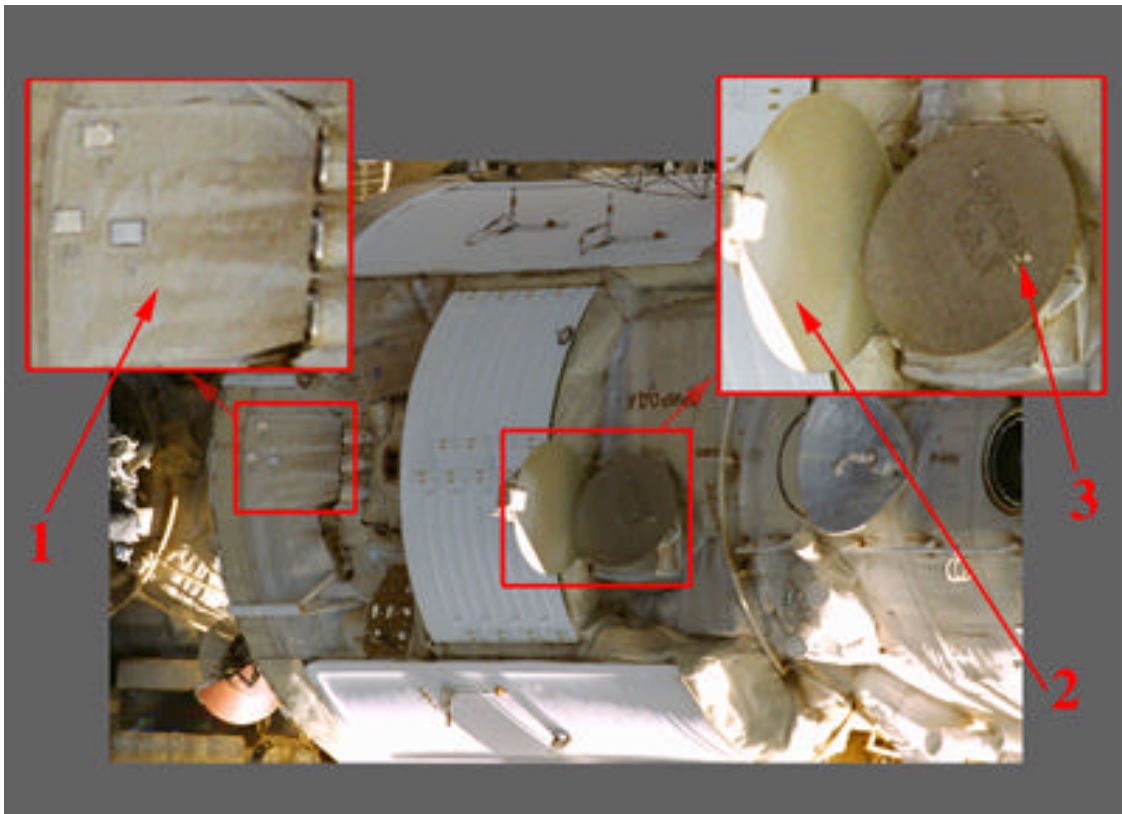


**Figure 3.20 -XB Deposition and Damage on Priroda**

---

#### 4. DOCKING MECHANISM ASSESSMENT

Imagery obtained during STS-86 was examined to verify the condition of the docking mechanism in preparation for STS-89. The imagery included film photography and video acquired during approach and backaway. However, close-up film photography of the docking mechanism was not obtained during either approach or backaway.

Docking occurred during a night pass on STS-86. The video imagery obtained with the Orbiter Docking System (ODS) centerline camera during approach showed the centerline docking target to be in good condition. However, there were significant reflections in the video when the docking latches were in the field-of-view. The video imagery was not suitable for assessment of the docking latches, alignment guides, electrical connectors, or retroreflectors. However, a view taken with the 70 mm camera and telephoto lens during approach (prior to darkness) was sufficient to show the capture and structural latches were in proper position and the centerline and non-axial targets were in good condition. The retroreflectors and electrical connectors appear to be in good physical condition. However, the imagery was not of sufficient resolution to detect discolorations that might exist. The image is shown in Figure 4.1.

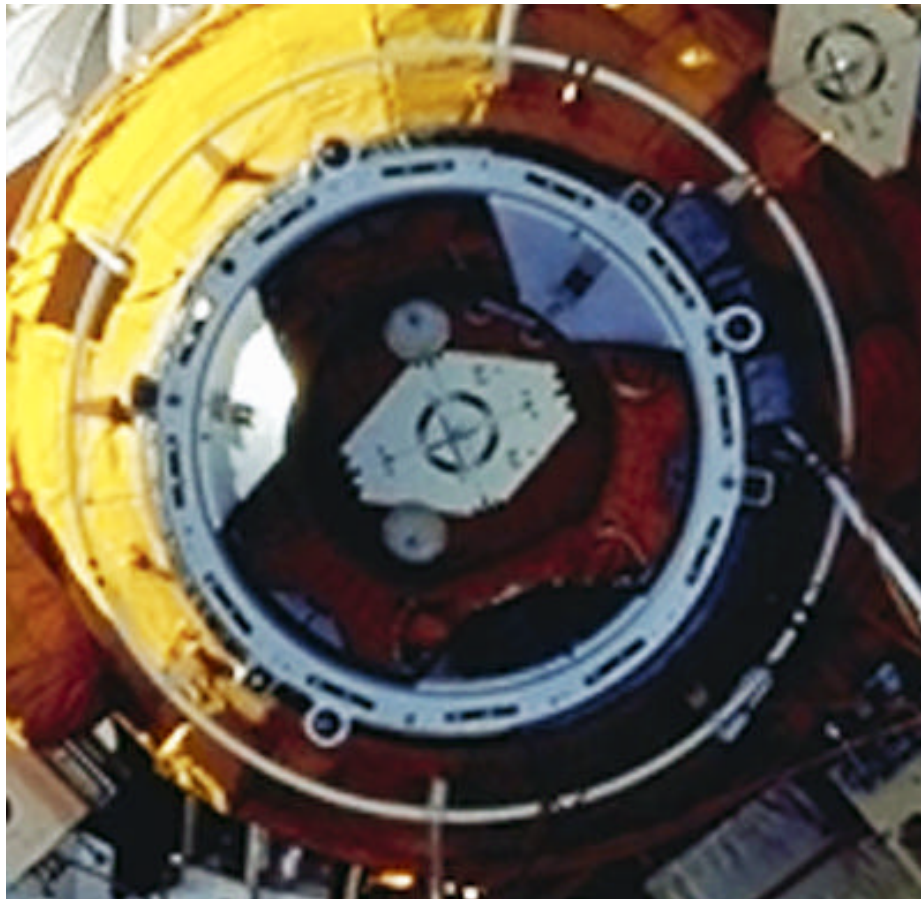


**Figure 4.1 Photo of Docking Mechanism during Approach**

---

Undocking and backaway also occurred during a night pass. A new centerline docking target was installed during STS-86. The video imagery obtained with the ODS Centerline camera during backaway showed the newly-installed centerline docking target to be in good condition. As during the docking, reflections prohibited use of the video imagery for assessment of the docking latches, alignment guides, electrical connectors, or retroreflectors. However, a view taken with the 35 mm camera and telephoto lens during backaway (after sunrise) was sufficient to show the capture and structural latches were in proper position and the centerline and non-axial targets were in good condition. The photographic image is shown in Figure 4.2.

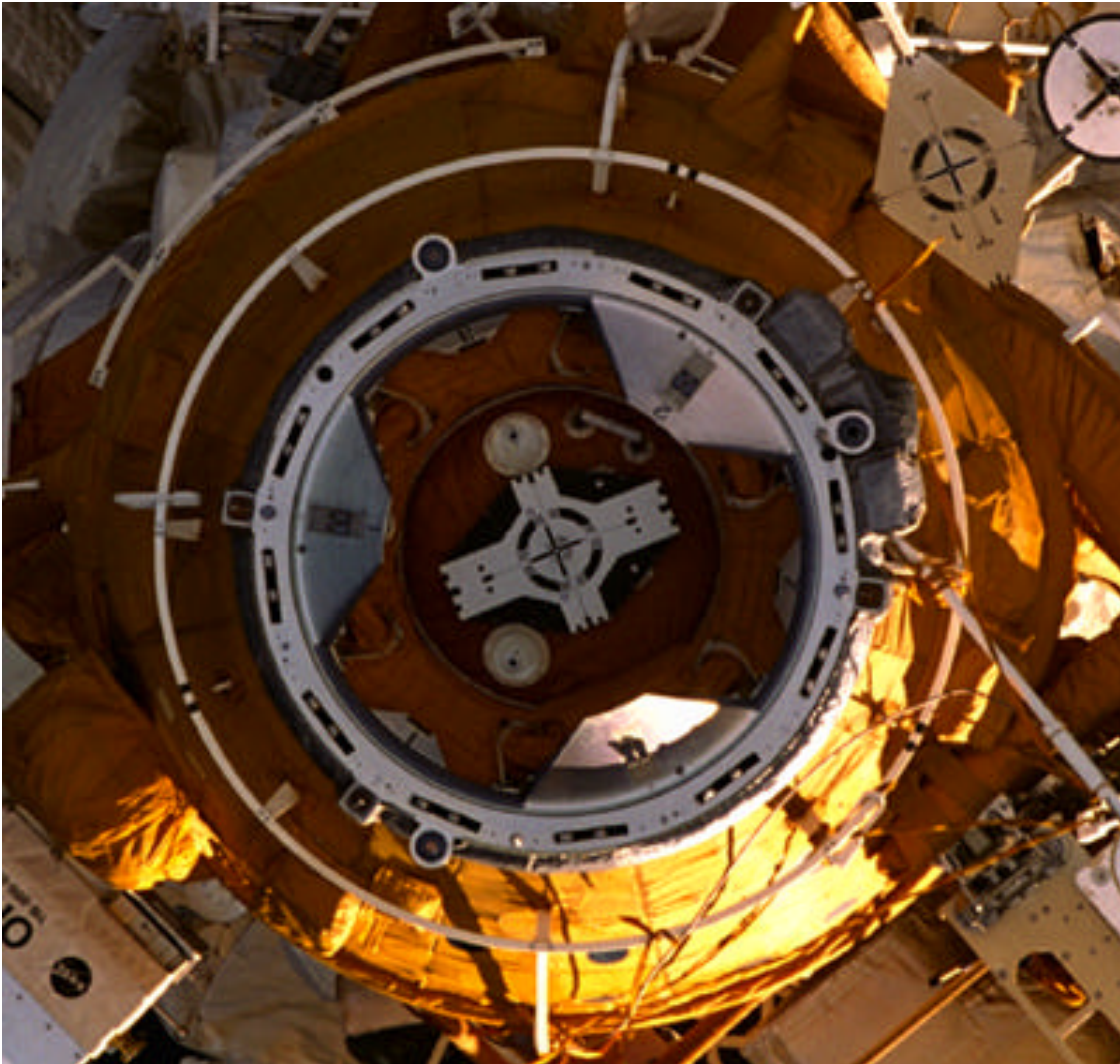


**Figure 4.2** Photo of Docking Mechanism during Backaway

---

## 5. SOLAR ARRAY MOTION

### 5.1 Mir Structural Dynamics Experiment Solar Array Motion

The Mir Structural Dynamics Experiment (MiSDE) is a risk mitigation experiment for the International Space Station (ISS). The purpose of the experiment is to obtain dynamic structural response data of the Mir. Accelerometers are placed throughout the Mir and measure accelerations in three dimensions as the Mir responds to a variety of dynamic load stimuli. Crew exercise activities on-board the Mir, and timed thruster firings from the Shuttle and Mir, are the most notable sources of perturbation. In addition to the accelerometers, video of solar array motion is captured during the timed thruster firings for correlation with the accelerometer response. Imagery analyses of solar array motions are performed in support of MiSDE to estimate the deflections and frequencies of the arrays due to docking, undocking, and by thruster firings during the docked phase.

On approach and docking on STS-86, PLB camera A was used to capture motion of the Base Block SP#2 solar array. During the pre-mission planning to acquire the docking video, it was anticipated that the array motion would be appreciably greater than the relative motion between the Orbiter and Mir. During the mission, the motion of the array was small and was difficult to separate from the relative motion during soft docking. The relative motion was caused by a small misalignment between the Orbiter and the Mir at the time of docking. This caused a greater movement of the Mir in the camera field-of-view. Since discrimination and separation of the array motion amplitude and frequency from the relative motion on the acquired video would require lengthy analysis, and would yield results which would have large errors, measurement of the array motion was not performed.

During the docked phase of STS-86, both Orbiter and Mir thrusters were fired to induce motion in Base Block SP#2. Barely-perceptible motion was noted in one test sequence. An automated point-tracking algorithm was used to analyze a small section of this sequence. The results from the small section analyzed show a maximum peak-to-peak displacement of approximately 0.10 inches. Error calculations place an uncertainty on this measurement of about  $\pm 0.10$  ( $1\sigma$ ) inches. Given that the magnitude of the measured motion is less than the uncertainty in the measurement, the displacement of the array could not be accurately determined.

### 5.2 Cooperative Solar Array

The JSC Structures and Mechanics Division requested that data be acquired and analyzed of the Cooperative Solar Array (CSA) truss, deployed on the -ZB array attach point of the Kvant module, to obtain measurements of the truss response to applied loads from Orbiter thrusters during undocking and separation. On STS-86, video was recorded during undocking using the Intensified TV Camera (ITVC) with a light-emitting diode (LED) illuminator in operation to compensate for the low light conditions. Figure 5.1 shows a typical camera view from PLB camera B position. The recorded CSA motion was very

---

small compared to the camera motion from loads imparted by the undocking sequence. If there had been significant motion of the array, the frequency of the motion could have been separated from other motions, such as the camera motion, in the frequency domain. However, the motion amplitude and frequency of the array could not be separated from the motion of the camera. Therefore, measurement of the array motion was not possible.



**Figure 5.1 Representative Video Frame of CSA during Undocking**

### **5.3 Thermally-Induced Motion of the Base Block Solar Array**

Since the first Shuttle docking to Mir (STS-71), several solar array motion events have been analyzed which were the results of external stimuli, such as thruster firings or crew-induced motion. During STS-86, an Orbiter payload bay camera was incidentally pointed at the end of a Mir solar array and captured deflection of the array as the Mir/Orbiter stack entered a night pass. It appeared this deflection was thermally-induced. This is the first known time imagery of this phenomenon had been captured. In fact, although some thermal deflection of the array could be expected, array loads models currently do not account for this effect, in part since the magnitude of the effect was not previously known.

Video data of Base Block SP#2 array motion was acquired during the ground-based video survey of Mir conducted from the Instrumentation and Communication Officer (INCO) console in the Mission Control Center (MCC). Payload bay camera A was used to record the motion, since it was positioned almost directly below the array (Figure 5.2). The camera was configured to capture entire sunrise and sunset sequences. A total of seven sequences were recorded. Five of the acquired video sequences were selected for analysis. Figure 5.3 shows a representative video frame of Base Block SP#2 during a day pass. The total deflection of the array during a transition from the day to night is illustrated in red.

---

To perform the deflection analysis, one frame of video was used at the start and end of each sunrise/sunset sequence. The point to be tracked on the array, an appropriate scale, and the time span between frames was determined from the captured frames of video. The beginning and ending frames for each sequence were imported into an image processing package and the location of the tracked point was measured in both frames. This data was then imported into a spreadsheet which computed the deflection and determined the error in the measurement.

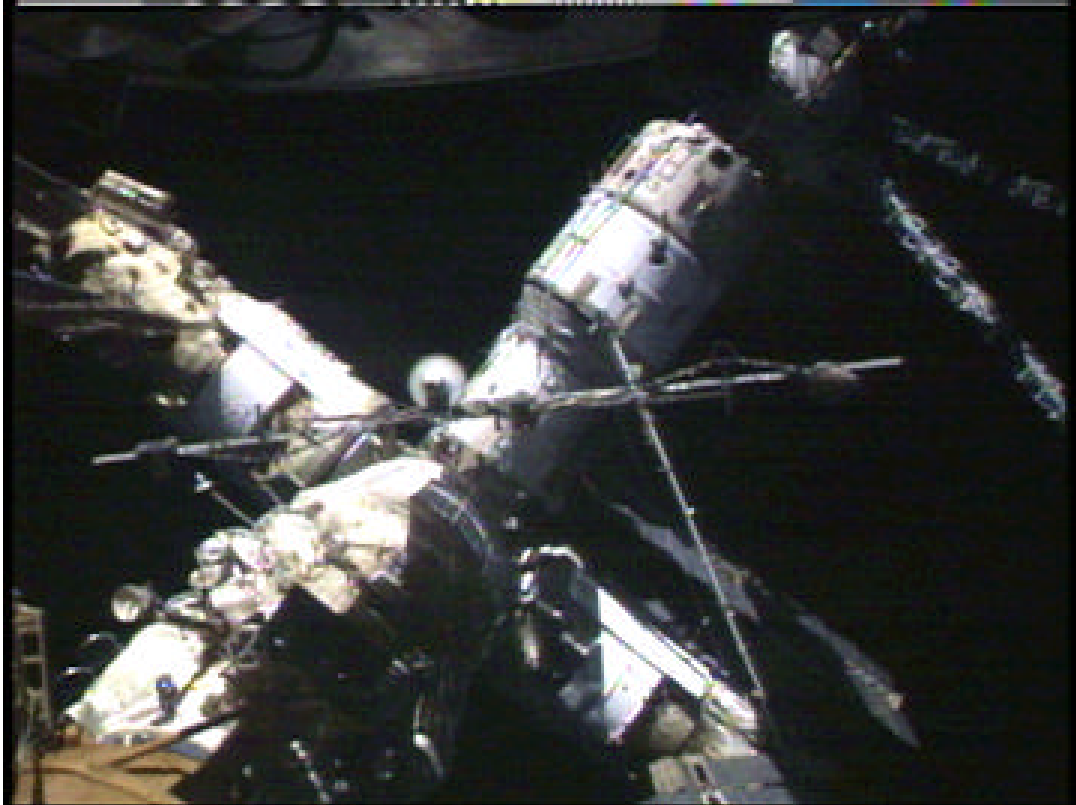


**Figure 5.2 Overview of Base Block SP#2 from Camera A**

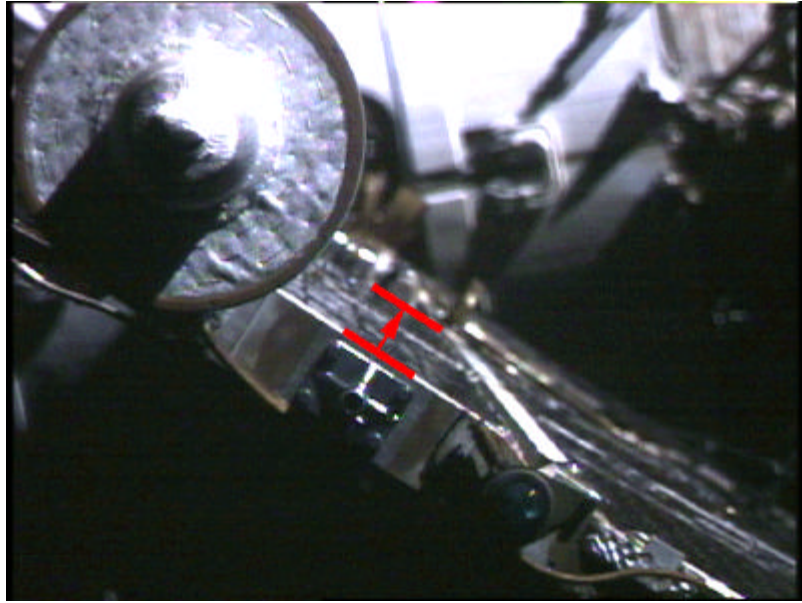


**Figure 5.3 Representative Video Frame of Base Block SP#2 during a Day Pass**

The scale used to measure the solar array deflection was calculated from the thickness of the array. Since the thickness of the array could not be determined from available drawings, it was calculated to be  $3.7 \pm 0.6$  inches by scaling from the array width (152.4 inches). The uncertainty in the array thickness calculation was redetermined by making repeated, independent measurements of the edges of the array. The standard deviation of the difference in thickness from measurement to measurement was taken as the uncertainty in the array thickness. This uncertainty was assumed to be the same for each sequence. The error in the measured distance traveled by the array, as taken from the difference in beginning and ending frames, was calculated as the square root of twice the square of the standard deviation of the array thickness.

The resulting deflection measurements for the five sequences are presented in Table 5-1. Deflections during day-night transitions (i.e., cooling) are noted with a minus (-) sign, while deflections during day-night transitions (i.e., heating) are noted with a plus (+) sign. The average values of the sequences are also shown.

---

**Table 5-1 Analysis Results of Thermally-Induced Motion**

Analysis Sequence	Transition	Deflection (inches)	GMT Start Time (dd:hh:mm:ss)	Elapsed Time (seconds)
1	Day-night	-2.7±0.6	273:06:08:30	93.2
2	Day-night	-2.2±0.6	273:08:11:53	53.3
3	Day-night	-2.0±0.6	273:09:13:11	48.2
4	Night-day	+4.0±0.6	273:09:44:12	175.8
5	Night-day	+3.6±0.6	273:10:45:37	117.2
	Day-night Average	-2.3±0.6		64.9
	Night-day Average	+3.8±0.6		146.5

The most probable reason for the difference in day-night vs. night-day measurements is simply that the solar array could not be tracked or measured over a complete cycle, since the array is not sufficiently visible for roughly half of every orbit. Therefore, the continued motion of the array throughout the orbital pass could not be measured from the available video. Further, as only a portion of any given orbit is visible, any deflection rate information derived from the data used in this analysis would assume the rates were constant. This may or may not be the case. Expanded study of this type of array motion on future missions could produce a more accurate characterization of this thermally-induced phenomena.

---

## 6. DEBRIS DURING DOCKING OPERATIONS

Small pieces of debris are normally seen on orbit during most Shuttle missions. Previous Shuttle missions to Mir have revealed extensive debris originating from the interface of the Mir Docking Module and the Shuttle ODS just after first contact was made and sunrise occurred. The low sun angle provides background illumination which facilitates visibility of the small debris. Most small debris is believed to be paint flakes or ice. Similar debris was not observed in the STS-86 video because docking occurred prior to sunrise. Debris was noted during four phases of the STS-86 mission: Approach, backaway, station-keeping, and fly-around. Size and velocity estimates for the debris observed were not made since the distance of the debris from the camera cannot be determined.

The ODS centerline television camera did not show any debris during the time of docking. However, it did detect debris prior to docking. The first piece of debris was noted moving away from the Payload Bay (PLB) approximately 52 minutes prior to soft dock. Another piece was captured by the centerline camera approximately 44 minutes prior to docking, as it traveled in front of Mir and changed direction abruptly by approximately 90 degrees, probably due to thruster firings. This debris and its trajectory are illustrated in Figure 6.1. Other pieces of debris were noted in the area surrounding the ODS approximately 27 minutes prior to soft dock. One piece of debris, recorded by camera D approximately 19 minutes prior to docking, appears to come into the ODS from the direction of Mir and may have made contact with the Orbiter, as shown in Figure 6.2. However, contact was not observed and none of the other pieces of debris observed prior to docking were seen to make contact with Shuttle or Mir hardware.

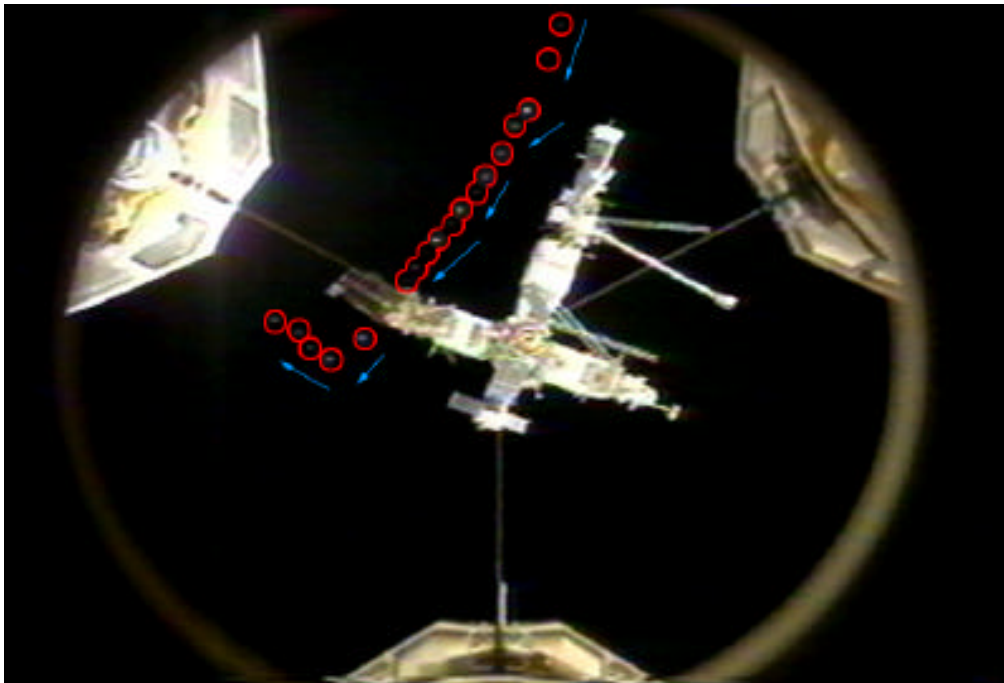


**Figure 6.1 Debris Observed Prior to Docking at GMT 270d:19h:17m:08s**



**Figure 6.2 Debris near ODS Prior to Docking at GMT 270d:19h:41m:35s**

During the 20 minutes following undocking, numerous pieces of debris were noted. Figure 6.3 shows a view from camera B and a large piece of debris passing over the PLB. A few pieces were noted passing between the Shuttle and Mir 40-60 minutes after undock. Most of the debris noted during this phase are barely visible.



**Figure 6.3 Debris after Undock at GMT 276d:17h:46m:53s**

---

Several pieces of debris were noted during station-keeping. Among these is the rope-like debris illustrated by the camera D video still frame shown in Figure 6.4. This debris moved parallel to the XB axis of Mir 48 minutes after undock. Other debris was noted passing either behind or in front of Mir.

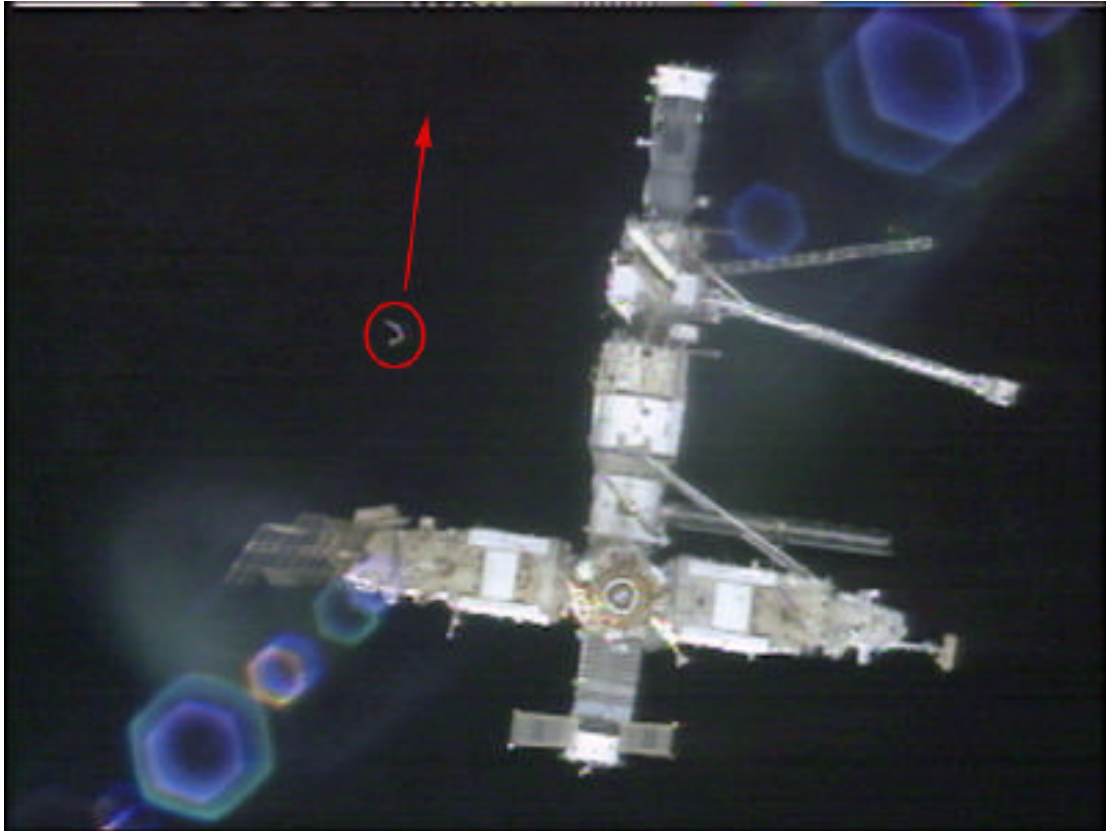


**Figure 6.4 Rope-like Debris noted during Station-keeping at GMT  
276d:18h:11m:28s**

Only two pieces of debris, other than those associated with the Spektr gas release event, were noted during fly-around. Both of these appeared small and were noted approximately 2 hours and 16 minutes after undock. These two pieces traveled the same path parallel to the XB axis in the +XB direction and were observed approximately one minute apart.

---

## 7. MIR ENVIRONMENTAL EFFECTS PAYLOAD ASSESSMENT

The MEEP experiment, which was attached to the Mir Docking Module during STS-76, was retrieved by the STS-86 crew during an EVA. The purpose of the MEEP experiments has been to study the frequency and effects of space debris striking the Mir Space Station and to expose selected ISS materials to the effects of space and orbital debris. The experiment consists of four separate payloads: the Polished Plate Micrometeoroid & Debris (PPMD) Experiment, the Orbital Debris Collector (ODC), and two Passive Optical Sample Assemblies (POSA and POSA II). Imagery of the MEEP panels has been acquired on each of the Shuttle rendezvous missions since their installation to assess any changes to the panels. Each of the four experiments are identified in Figure 7.1, was taken during the STS-86 Shuttle approach to Mir.

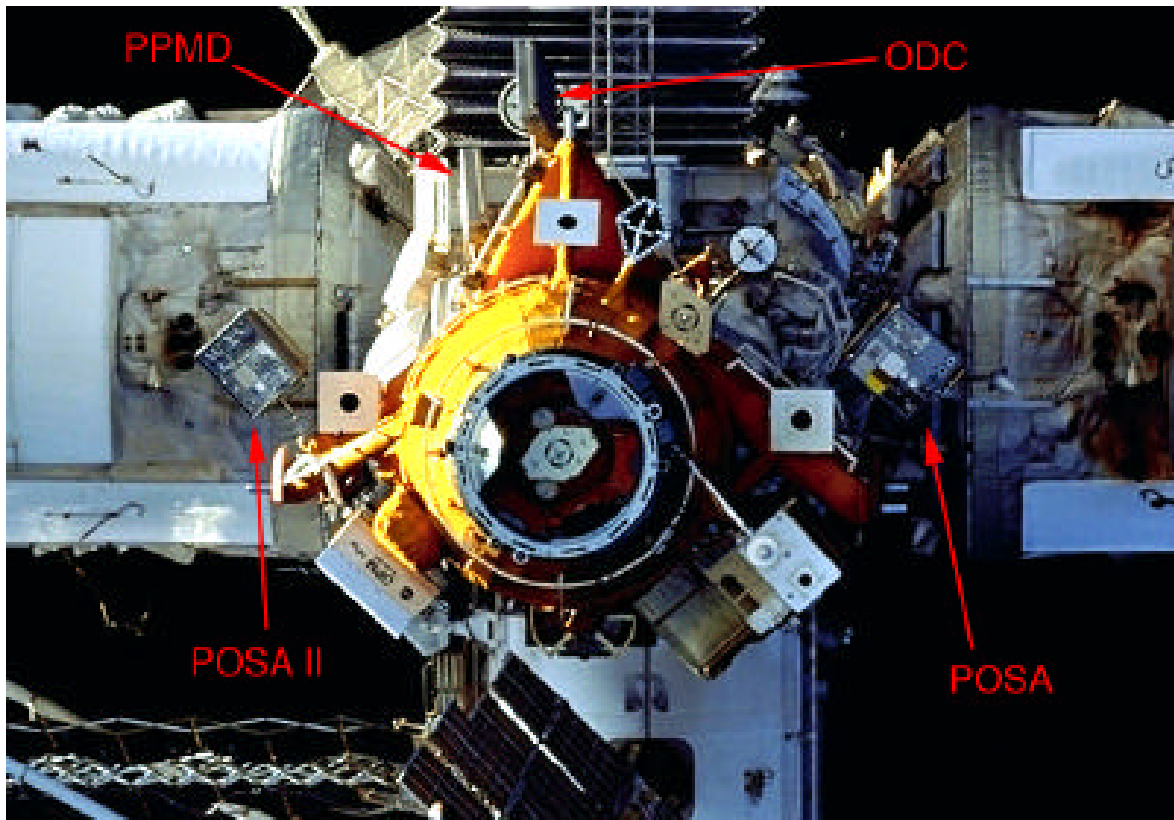


**Figure 7.1 STS-86 Image of Mir with MEEP Experiments**

Detailed, close-up images of the panels were taken with the 35 mm camera during the EVA to retrieve the four experiment payloads. Figure 7.2 shows the PPMD and ODC experiments to be in good condition. Figure 7.3 shows evidence of possible contamination of POSA II in the form of numerous small brown spots visible on the outer casing and on areas within the panel. Preliminary results of analysis of the MEEP panels presented at the ISS/Mir Space Environment Effects Meeting of January 13, 1998 suggest

---

these deposits may have originated from multiple Orbiter waste water dumps and/or from Progress condensate waste leaks. Imagery of POSA II taken on STS-84 showed no indications of this type of contamination, however, these earlier images were of a lower resolution than the STS-86 EVA photography.



**Figure 7.2 EVA Image of PPMD (left) and ODC (right)**

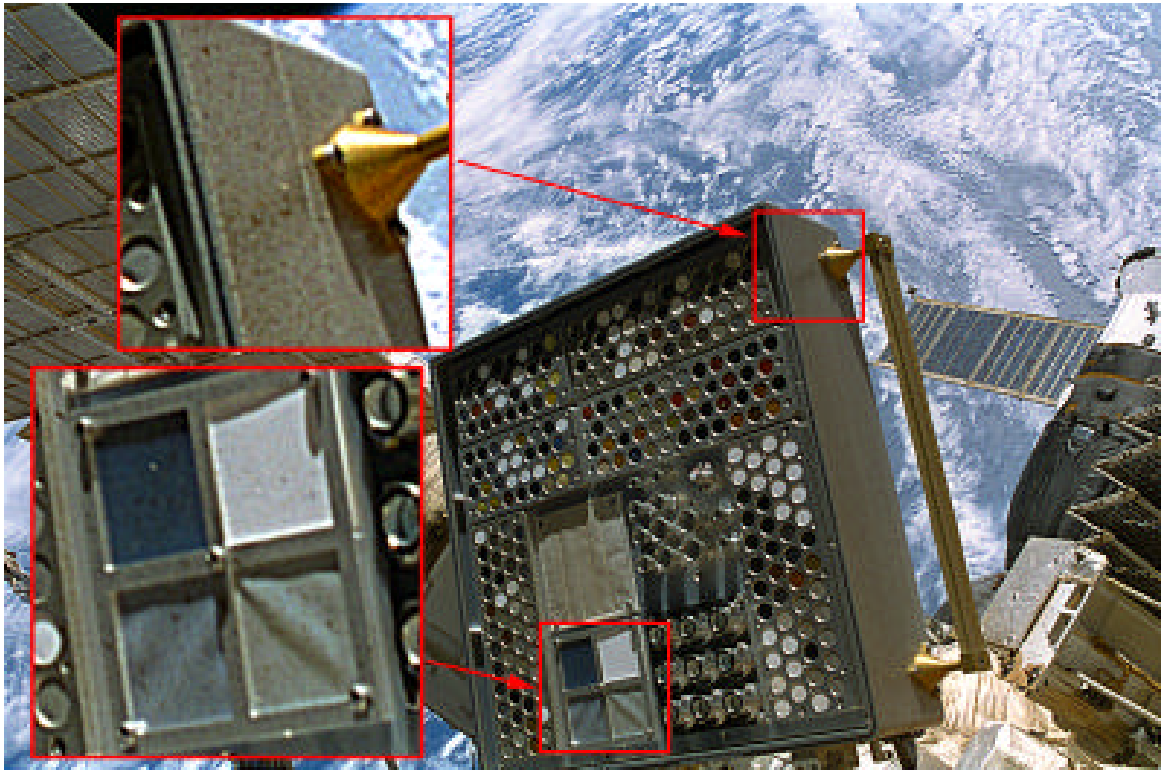


**Figure 7.3 EVA Image of POSA II Showing Contamination**

Images of the space-facing side of POSA taken from the aft flight deck window show what appear to be small white deposits on some of the circular, optical test specimens in the panel. The nature of these deposits is still under investigation. A review of the imagery of past missions shows that these deposits began appearing as early as the STS-79 mission. Figure 7.4 is a composite of images from missions STS-79 through STS-86, each showing an identical section of the POSA panel containing the deposits. All were taken from the aft flight deck window and all were taken with the 35 mm camera except for the STS-81 image which was taken with the 70 mm Hasselblad. The images in Figure 7.4 have been adjusted to a common scale to account for the varying focal length lenses that were used.



STS-79



STS-81



STS-84



STS-86

**Figure 7.4 Images of the Same Section of POSA Taken on Four Separate Shuttle/Mir Missions**

---

## 8. POSITION OF THE KURS ANTENNA ATTACHED TO THE DOCKING MODULE

Between STS-79 and STS-81, a Kurs antenna was attached to the Mir Docking Module. This Kurs antenna extends toward the Shuttle forward bulkhead as shown in Figure 8.1. The JSC Structures and Mechanics Division (SMD) requested that an analysis be performed to determine the position of the tip of the antenna from STS-81, STS-84, and STS-86 imagery. This position information will assist SMD in determining the clearances between the antenna and the Shuttle Payload Bay forward bulkhead. The STS-81 and STS-84 results were included in references 6 and 7. The following describes the STS-86 analysis and results.

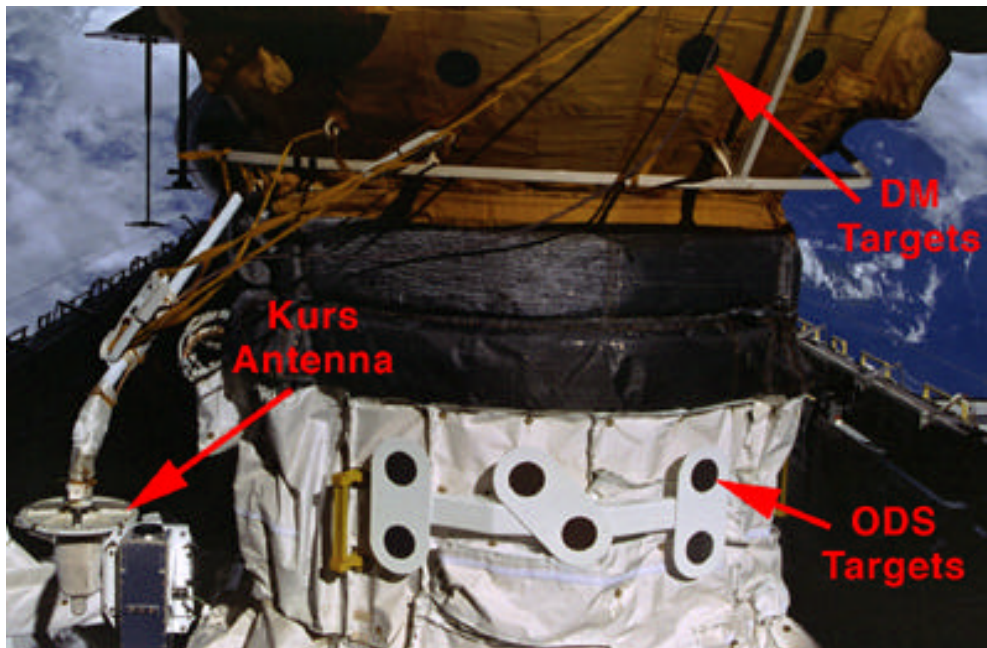


**Figure 8.1 Kurs Antenna as seen from the Shuttle Flight Deck on STS-84**

Standard photogrammetric techniques were used to determine the location of the Kurs antenna. The same techniques were used for the STS-81, STS-84, and STS-86 analyses. Two overlapping video images of the antenna were used to perform a 3-dimensional triangulation to determine the position of the tip of the antenna in the Shuttle Structural Coordinate System (SSCS). The ODS targets and the Docking Module targets of the Orbiter Space Vision System (OSVS), shown in Figure 8.1, were used to establish the camera pointing angles for the two STS-86 video images used in the analysis. These two images from Shuttle PLB Cameras A and D are shown as Figures 8.2 and 8.3 respectively.

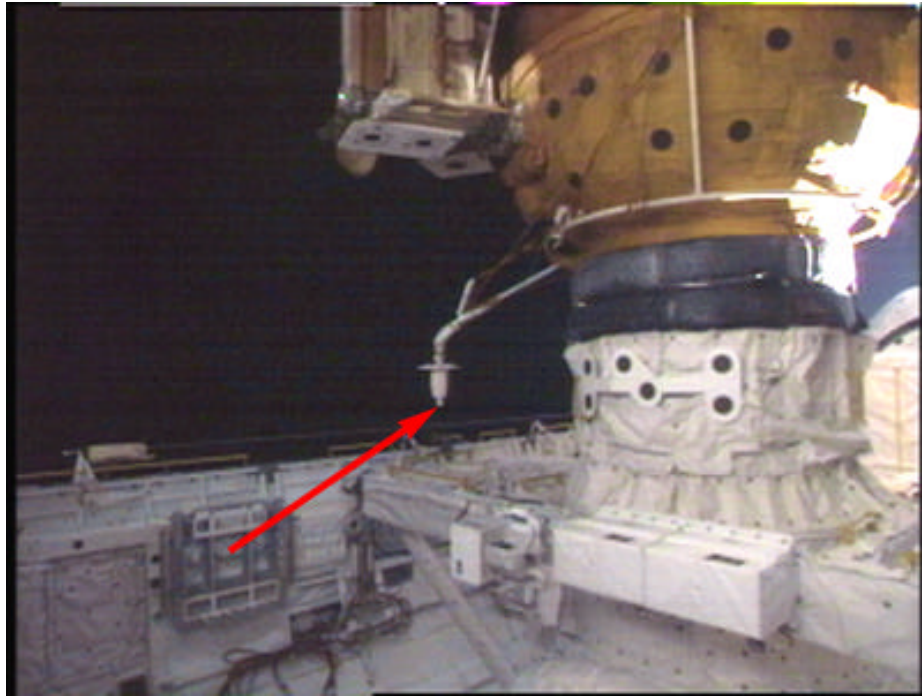


**Figure 8.2 Kurs Antenna as seen from Payload Bay Camera A**

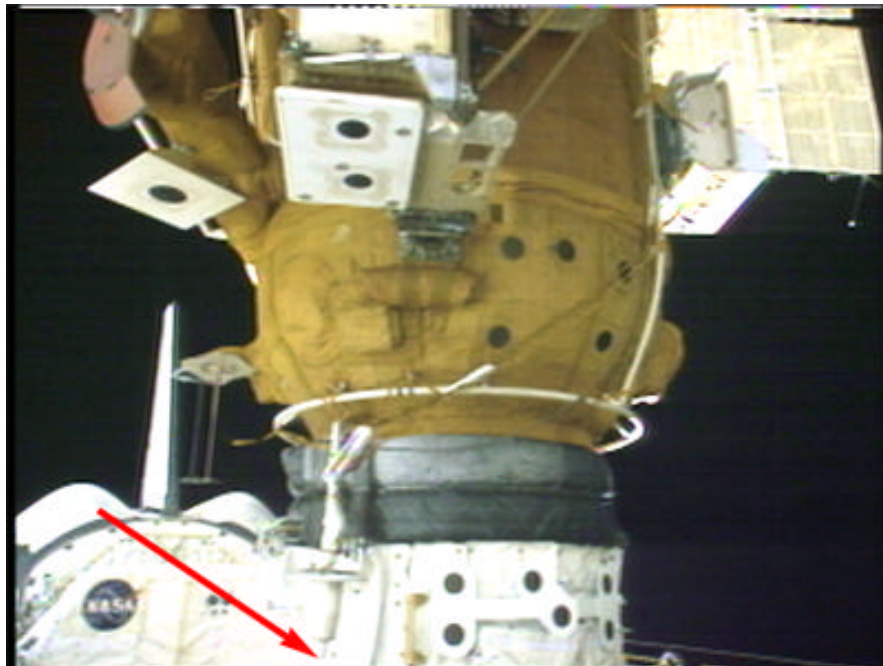


**Figure 8.3 Kurs Antenna as seen from Payload Bay Camera D**

The results from the STS-86 analysis are given in Table 8-1. The STS-81 results, the STS-84 results, and the expected coordinates based on data obtained from the Space Shuttle Program Integration Engineering Office are also in the table. The estimated positions from STS-81, STS-84, and STS-86 analyses are accompanied by an uncertainty estimate derived from a standard Monte Carlo error estimator. The STS-86 results indicate a clearance of 109.8 inches between the tip of the antenna and the Shuttle forward bulkhead. The STS-81 and STS-84 clearances were calculated to be 109.4 and 109.6 inches respectively.

**Table 8-1 Coordinates of Kurs Antenna Tip**

	SSCS Coordinates (inches)		
	$X_o \pm 3\sigma$	$Y_o \pm 3\sigma$	$Z_o \pm 3\sigma$
Expected Position	683.4	40.5	439.1
STS-81 Position	$685.4 \pm 2.1$	$42.3 \pm 1.2$	$439.3 \pm 0.9$
STS-84 Position*	$685.6 \pm 1.7$	$40.8 \pm 1.1$	$439.1 \pm 0.9$
STS-86 Position	$683.8 \pm 1.8$	$43.2 \pm 1.1$	$438.0 \pm 0.9$

\*Values are revised from results in the STS-84 report. Reanalysis of STS-84 data changed the  $X_o$  coordinate from 686.1 to 685.6 inches and the  $Y_o$  coordinate from 40.5 to 40.8 inches. The  $Z_o$  coordinate did not change. The  $3\sigma$  errors are unchanged.

The Monte Carlo error estimator attempts to define the maximum expected deviation of the estimated position of the antenna tip from its true position. The primary contributors to the input errors are the errors in the digitized image positions of the tips. The resolution of the video imagery has a large effect on the ability to accurately establish the digital image positions, but resolution of a given image is affected by multiple factors, many of which cannot be accounted for in a simple Monte Carlo error analysis. Because of this, “worst case” variances are input to the Monte Carlo analysis which cause the error estimates of the Monte Carlo analysis to be conservative.

As an additional error assessment, the photogrammetric technique used to estimate the Kurs antenna position was also used to estimate the position of each of the OSVS targets used. The results of these analyses were compared to the ground-surveyed position of the OSVS targets, which have a  $3\sigma$  accuracy of  $\pm 0.09$  inches. The  $3\sigma$  results of the differences between the estimated and surveyed positions of the OSVS targets were:  $3\sigma(X_o) = \pm 0.84$  inches;  $3\sigma(Y_o) = \pm 0.60$  inches;  $3\sigma(Z_o) = \pm 0.34$  inches. Comparison of these values with the error values for the positions given in Table 8-1 further indicates the error values in Table 8-1 are conservative estimates of the true error.

---

A pairwise statistical comparison was performed on the position of the antenna for each mission. The results of this comparison would suggest that the antenna has slightly changed position between STS-84 and STS-86. The actual statistical analysis can be found in reference 8.

---

## 9. IMAGERY EVALUATION

This section discusses the overall quality of the film and video data obtained during STS-86 for DTO-1118. The scenelist of flight films and an index to videotapes are included as Appendices C and D. Appendix E is a list of image sources for the imagery in this report. Appendix F shows the configuration of STS-86 cameras.

Most DTO-1118 objectives and customer targets were obtained.

Use of the 400 mm lens during the fly-around provided excellent detailed photography of the damage to Spektr. Other fly-around photography provides coverage of areas of the Station not obtained on previous missions.

Imagery acquired of Mir surfaces during STS-86 consisted of the following:

- Approximately 54 hours of downlink and onboard video.
- 1180 frames of 35 mm film.
- 520 frames of 70 mm film.
- 10 Electronic Still Camera Images (ESC) images.

### 9.1 Still Photography Review

Approximately 66 frames of Hasselblad (70 mm) photography were acquired during approach. These images, captured with a 250 mm lens, provided an overview of all Orbiter-facing sides of Mir modules. Three overview images of the Mir docking mechanism were acquired during close approach. These images of the station were taken under poor lighting conditions since docking occurred at the beginning of a daylight pass. As on previous missions, limited overhead window access time during approach hampered imagery acquisition.

The STS-86 crew obtained large-scale, high-resolution photography of Mir surfaces while the Shuttle was docked. Imagery was taken from the Shuttle aft flight deck windows, the Spacehab window, and from Mir windows. This imagery was highly beneficial for analysis of the Kvant radiator, surfaces of the Base Block, and damage to the Spektr arrays and radiator.

Overview coverage of the Orbiter-facing sides of Kvant, Spektr, Kvant-2, Kristall and Base Block modules was obtained using the both the Hasselblad and Nikon cameras during the docked phase. The Hasselblad 70 mm camera with the 250 mm lens was used from a Base Block window to acquire detailed photography of the damaged Spektr array and radiator. In addition, excellent detailed coverage was acquired with the 400 mm lens on the Nikon 35 mm camera of the following Mir features :

- The Kvant end dome at the Base Block interface.
- Base Block surfaces.
- The EVA Cargo Boom attach points on the Base Block and Kvant-2.

- 
- Experiments on the end of Kvant-2.
  - The (-ZB) Spektr radiator.
  - The MEEP POSA panel.

Good detailed views of the Base Block SP #2, Kvant-2 SP #2, Spektr SP #2, and Spektr SP #4 were acquired. Photography acquired during the EVA provided 16 overview photographs of the MEEP panels. Overview photography of the Station was obtained with both the Nikon and Hasselblad cameras during backaway. Eighteen photographs of the Mir docking mechanism were taken.

Fly-around photography acquired with both the Hasselblad and Nikon cameras provides excellent detailed coverage of the damage to Spektr caused by the Progress collision. Good coverage of the Spektr surfaces was obtained from the start of the fly-around at the -XB, +ZB side of the module to the +XB, -ZB side at the end. The sunlight coming from the +XB direction throughout the fly-around greatly enhanced the quality of the photography. The quality of the imagery acquired was excellent except for photography from the 80-200 mm zoom lens on the Nikon, which appeared to have some motion blur and/or focus problems.

During the Spektr gas release, photography was acquired of two particles in the vicinity of Spektr. Three sequential Hasselblad frames captured two of the five particles which were seen during the gas release. Three sequential frames taken with the Nikon appear to capture the largest particle which was seen during the gas release. The Nikon frames appear to have some motion blur.

Other fly-around photography provides coverage of areas of the Mir Station not obtained on previous missions. These areas include the +ZB sides of the Base Block, Kvant, and Kvant-2. In addition, the +XB side of Kvant-2 was covered in much greater detail than previous missions. The photography taken during this mission greatly increases the number of areas of Mir which are photographed in good detail.

ESC imagery of Mir provided two views of Mir during the docked phase and eight during fly-around. These represented the only ESC frames taken of the external surface of Mir.

## **9.2 Video Review**

The centerline camera provided the first views of the Mir approximately 1 hour before docking. During the dark phase of the orbit, only the station onboard lights were visible.

Final approach and docking occurred during darkness. The video imagery obtained with the ODS centerline camera during approach showed the centerline docking target to be in good condition. Limited detail could be observed on the docking mechanisms due to glare reflected from the docking ring caused by the docking lights. Undocking and backaway also occurred during darkness. Once again, there was limited detail observed on the docking mechanisms due to glare.

---

An INCO-controlled video survey was performed during three crew sleep periods of the docked phase. All four PLB cameras were used in acquiring Mir survey imagery. This footage provided good coverage of the Orbiter-facing sides of the Spektr, Kvant-2, Base Block, Kristall, Kvant, Priroda, Soyuz and Progress modules. Coverage of the Spektr damage was minimal due to its location in relation to the PLB cameras. Video mapping of the Docking Module was performed to obtain close-up imagery of the OSVS targets. In addition, close-up views of the Kurs antenna were recorded.

The MiSDE was performed during the docked phase of STS-86. During Shuttle and Mir thruster firings, PLB cameras A and D were multiplexed and recorded motion at the tip of Base Block SP#2. PLB cameras B and C were multiplexed and recorded motion at the array attach point.

Array motion of Base Block SP#2 was visible during transitions between orbital day and night due to solar heating/cooling. This motion was observed and recorded during several transitions into both day and night as part of the INCO survey.

During backaway, the centerline camera provided views of the Mir docking interface area. For this Shuttle-Mir mission, the ITVC camera with an illuminator ring was used for acquiring video under low-light level conditions. The light ring produced enough light to effectively illuminate the CSA which was 90 feet away from the camera during backaway. Although the video image appears dark, an increase in the video gain setting during playback produces a good image of the array.

Acquiring video of the Spektr module and the associated gas release events was the primary objective of the fly-around. Coverage of these events was obtained from PLB cameras D (forward, starboard) and B (aft, port). Survey coverage of the Mir was obtained from camera D between gas release events. An analysis of the particles seen during the venting tests was performed and the report is included in Appendix B.

### **9.3 Crew Assessment**

The following is a summary of STS-84 crew assessment of the imagery acquisition. The summary is based on a debrief held on November 24, 1997.

- Preflight training was adequate to perform the DTO (two training sessions were held: familiarization and detailed).
- Diagrams and photos helped locate the desired target areas (the crew was provided with diagrams from the Russians which identified areas of possible damage on the Mir caused by the Progress collision). Detailed target lists were also useful.
- The location of a locker in the double Spacehab module made it very difficult to take the desired photographs of the Mir out the port aft window. A crew member had to remove the contents of a locker so that there was room for his head to look through the viewfinder.

- 
- During approach, it was difficult to acquire targets due to poor lighting and limited overhead window access time. Backaway conditions provided more window access time.

---

## 10. CONCLUSIONS AND RECOMMENDATIONS

### 10.1 Conclusions

Based on the analysis of STS-86 imagery, the following conclusions have been made:

- The damage to the Mir exterior caused by the Progress collision appears limited to the Spektr module and its appendages. No other areas of damage to Mir surfaces were observed in the STS-86 mission photography.
- The STS-86 fly-around of the Mir Station at 250 feet provided higher resolution photography than was acquired from past mission fly-arounds, which were flown at about 500 feet. A comprehensive understanding of damage to the Spektr module surfaces and appendages would not have been possible without the high-resolution fly-around photography. Much of the damaged areas on Spektr is not visible from the Shuttle during the docked phase. In addition, the fly-around provided an opportunity to increase the overall photographic coverage of the Mir Station external surfaces.
- The particles from the Spektr venting test appear detectable. Video recorded from payload bay camera D during the STS-86 Mir fly-around provided trajectory data on seven particles seen moving away from Spektr. However, the composition of the particles could not be determined from the video. Two-dimensional analysis of the trajectories of the particles indicate multiple points of origin.
- Measuring motion of solar arrays during solar thermal cycling is feasible. The edge-on view of Base Block SP#2 provided by payload bay camera A allowed for measurements of this motion which was as much as 4 inches during one of the day-night transitions.
- The imagery from the STS-86 mission substantially augmented the imagery from previous Shuttle/Mir missions. The combined imagery gathered from STS-63 through STS-84 missions provide significant information from which an assessment can be made on the effects of the space environment on an orbiting platform.
- The imagery surveys continue to provide new details on the effects of the space environment on the Mir Space Station. These effects are observed on structures and surfaces regardless of the amount of time they have been on-orbit. In addition, the imagery surveys have created a temporal record of the Mir Space Station's external surfaces.
- The amount of high-resolution imagery is increasing with each additional mission. Although major Mir surface changes (except for the Spektr damage) were not observed on STS-86, there is improved identification of smaller features and definition of surface characteristics, including discoloration, micrometeoroid/orbital debris damage, and surface and structural anomalies.
- The analysis of structural motion from video acquired on STS-86 during docking and undocking was hampered by several factors: motion of the cameras, poor lighting, poor video quality, and small amplitude of the solar array motion.

---

## 10.2 Recommendations

Based on the analyses documented in this mission report, crew comments during training and post-mission debriefs, and evaluation of the STS-86 and prior mission imagery, the following recommendations are made for the final Shuttle/Mir mission (STS-91) and upcoming ISS missions:

- For any future leak detection tasks such as the Spektr Venting Test on STS-86, to be performed using standard Shuttle equipment during a fly-around, the following recommendations are made:
  - (a) The Orbiter should station-keep relative to the Station shortly before, during, and shortly after each gas release. Station-keeping will help in the analysis of particle trajectories by providing a stable viewing perspective during the events.
  - (b) Two CTVC cameras should be used to view the module. The amount of noise contained in the ITVC signal made it less useful than expected.
  - (c) If possible, a multiplexed view (one combining simultaneous signals from two different cameras) should be recorded in addition to the normal, non-multiplexed, camera views. This would ensure that, in the event that a debris particle is observed in both views, the views will be exactly synchronized. Such synchronization is necessary for a three-dimensional analysis of the trajectories of any observed debris particles. The use of multiplexed views, however, limits each camera view to only half the normal field-of-view.
  - (d) Still photography is recommended in the event gas or ice plumes form, because of the greater detail that still photography can provide. In-frame timing is required for establishing a timeline of events captured on film.
- The Nikon with 400 mm lens should be the primary camera/lens combination for survey imagery acquisition. The higher resolution of this system provides greater detail of information during approach, while the Orbiter is docked, during backaway, and during fly-around.
- Universal Time Code (UTC) is required as a standard on all video recordings in order to correlate mission related events. On-orbit this is accomplished by inserting the time in the vertical interval.
- Crew time must also be allotted for set up of the video cameras prior to acquisition of planned structural dynamics tests. Set-up during daylight hours should be mandatory.
- INCO-controlled payload by video cameras should continue to be used to perform surveys during crew sleep periods. This has been the most effective way to obtain survey video coverage and also allows real-time decisions to be made on target acquisition.
- The need for bracketing exposures when acquiring imagery should continue to be emphasized. The bracketed exposures provide for additional detail in imagery with high contrast.
- The crew should continue to be made aware of lighting conditions that highlight surface features. Lighting angles oblique to Station surfaces convey textural information that would otherwise remain hidden.

- 
- The large amount of DTO-1118 photographic and video data collected over the entire Phase 1 program provides significant amount of information on the Mir Station. Each of the mission reports have focused, for the most part, on specific topics based on the data gathered during that mission alone. However, there is much more information which could be extracted from this data with further analysis, such as, a complete mapping and characterization of MMOD strikes on solar arrays from available photography, a mapping of discoloration to diagrams of the Mir modules, and a detailed analysis of all solar array motion observed.
  - Most assessment of surface discoloration/deposition in DTO-1118 mission reports have been qualitative due to a lack of controlled data collection conditions. Development of colorimetry standards for data collection is necessary for quantitative measurements to be made.
  - The focus of DTO-1118 has primarily been on the study of outer surfaces and appendages of Mir, with analyses on the effects of the space environment on external surfaces, and analyses of the dynamic effects of structures and appendages. A complementary internal survey of a space station would provide an integrated view of the station for long duration crew member training, documentation of hardware configurations, and a temporal record of the condition of station components if the survey is repeated at some interval.
  - The DTO-1118 experiences for imagery acquisition and analyses should be applied to the International Space Station program. Specific benefits arise from continual imagery acquisition starting with on-orbit close-out imagery and periodic imagery surveys. Each on-orbit viewing perspective (approach, docked, separation, fly-around) provides differing types of complementary information.

---

## 11. REFERENCES

1. JSC-27246, NASA/RSC-E Joint Report, Mir Photo/TV Survey (DTO-1118): STS-63, August 28, 1995.
2. JSC-27355, NASA/RSC-E Joint Report, Mir Photo/TV Survey (DTO-1118): STS-71, January 16, 1996.
3. JSC-27649, NASA/RSC-E Joint Report, Mir Photo/TV Survey (DTO-1118): STS-74, November 20, 1996.
4. JSC-27525, Mir Photo/TV Survey (DTO-1118): STS-76 Mission Report, July 30, 1996.
5. JSC-27761, Mir Photo/TV Survey (DTO-1118): STS-79 Mission Report, March 28, 1997.
6. JSC-27932, Mir Photo/TV Survey (DTO-1118): STS-81 Mission Report, July 11, 1997.
7. JSC-28047, Mir Photo/TV Survey (DTO-1118): STS-84 Mission Report, September 1997.
8. SN-98-007, Assessment of STS-89 Kurs Antenna Position, March 3, 1998.

---

## 12. ACRONYMS & ABBREVIATIONS

CSA	Cooperative Solar Array
CTVC	Color Television Camera
DM	Docking Module
DTO	Detailed Test Objective
ESC	Electronic Still Camera
EVA	Extra Vehicular Activity
GMT	Greenwich Mean Time
INCO	Instrumentation and Communication Officer
ITVC	Intensified TV Camera
IS&AG	Image Science & Analysis Group
ISS	International Space Station
JSC	Johnson Space Center
LMES	Lockheed Martin Engineering and Sciences
MCC	Mission Control Center
MEEP	Mir Environmental Effects Payload
MiSDE	Mir Structural Dynamics Experiment
MMOD	Micrometeoroid and Orbital Debris
NASA	National Aeronautics & Space Administration
ODC	Orbital Debris Collector
ODS	Orbiter Docking System
OPM	Optical Properties Monitor
OSVS	Orbiter Space Vision System
PLB	Payload Bay
PPMD	Polished Plate Micrometeoroid & Debris
POSA	Passive Optical Sample Assembly
POSA II	Passive Optical Sample Assembly II
RSA	Reusable Solar Array (same as MSA)
RSC-E	Russian Space Center-Energia
SMD	Structures and Mechanics Division
SMPTE	Society of Motion Picture and Television Engineers
SP	Solar Panel
SSCS	Shuttle Structural Coordinate System
STS	Space Transportation System
UTC	Universal Time Code

## **Appendices**

**Appendix A: Preliminary Spektr SP#1 Geometric  
Deformation Analysis**

**Appendix B: Assessment of Spektr Venting Test Imagery  
Obtained During STS-86 Fly-around**

**Appendix C: STS-86 Film Scenelist**

**Appendix D: STS-86 Video Scenelist**

**Appendix E: Sources for Report Imagery**

**Appendix F: STS-86 Camera Layout**

**Appendix A: Preliminary Spektr SP#1 Geometric Deformation Analysis**  
SN3/Space Science Branch  
Image Science & Analysis Group

The IS&AG performed a geometric deformation analysis on Spektr Solar Panel (SP) #1, which was damaged after a collision by the Progress supply module. This geometry will assist the Structures and Mechanics Division in estimating the plume impingement loads.

A video tape showing the damaged Spektr SP#1 was obtained from a Soyuz fly-around on 8-15-97. An attempt was made to locate two frames parallel to the YB, -ZB and XB, -YB planes of the Mir body coordinate system (XB, YB, ZB). However, during the Soyuz fly around, no adequate views of Spektr SP#1 were found parallel to the XB, -YB plane. Although additional views of SP#1 could be seen at other angles, the viewing angle could not be accurately measured based on the available imagery. Therefore, only one video frame parallel to the YB, -ZB plane was used.

A single video frame was used to calculate the Mir coordinates of nine selected points on the Spektr SP#1. Each of these selected points of interest were located on the corners of the solar array panels. Based on visual inspection of the video, the four corners of each of the solar array panels of SP#1 appeared to be in approximately the same plane, so the nine points were deemed sufficient to define the geometry. The points analyzed are annotated in the video frame shown in Figure 1.

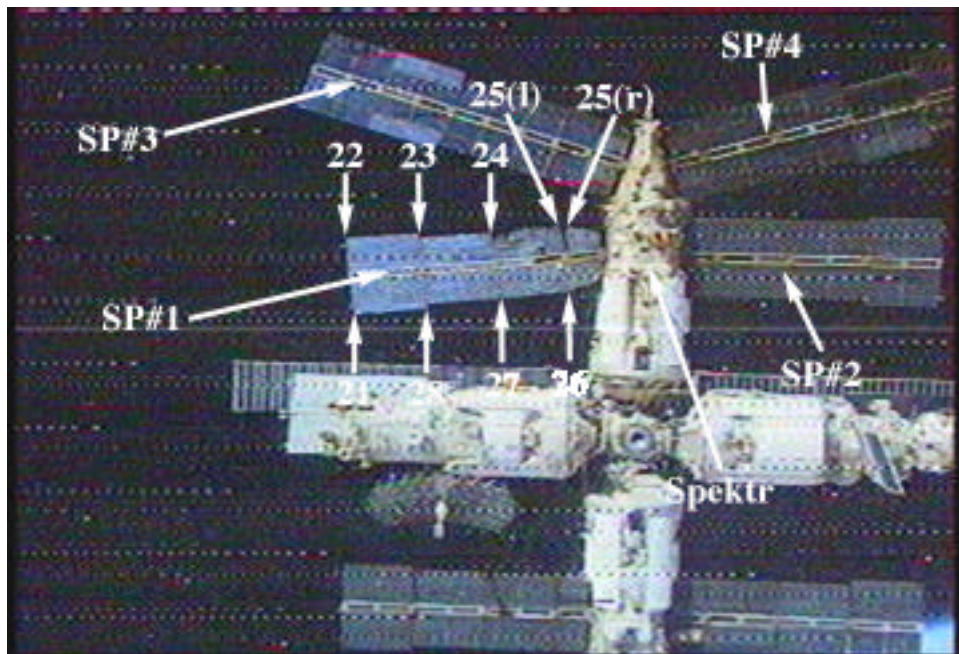


**Figure 1: Video Frame from Soyuz Fly-Around Used for Analysis**

The Mir body coordinates of the selected points on undamaged SP#1 and SP#2 arrays were obtained from a CAD model generated by Boeing North-American. The CAD model referenced SP#1 and SP#2 as being parallel with the YB, -ZB plane.

Several assumptions were made for the determination of the geometric deformation of the Spektr SP#1. The camera focal plane was assumed to be parallel with the YB, -ZB plane of the Mir coordinate system. The undamaged Spektr SP#2 were also assumed to be parallel with YB, -ZB plane. Further, SP#1 was assumed to have been generally rotated about its attach point.

The image was rotated 1.95 degrees counterclockwise to align the Mir YB, -ZB axes to the image plane x-y axes. After rotating the image, SP#2 was overlaid with horizontal and vertical lines to verify alignment with the image axes. Using the rotated image, several steps were performed in the analysis. Image coordinates of several solar panel corners on Spektr SP#1 and SP#2 and the two attach points, were collected. The scales of the image in both the YB and ZB directions were determined based on the horizontal and vertical distances of known coordinates on SP#2. In both the horizontal and vertical directions, the number of pixels between the upper right tip of SP#2 and the selected points on SP#1 was calculated. Using this number of pixels and the image scales, the YB and ZB components of the Mir coordinates of the selected SP#1 points were calculated. The attach point for SP#1 was calculated using a similar approach.

The XB components of the selected points of interest were computed based on the apparent angles that Spektr SP#1 was rotated out of the YB, -ZB plane and around the shaft of SP#1. The pitch angles, as rotated out of the YB, -ZB plane, were computed for each individual solar panel on SP#1. This was accomplished by computing the length of the panels in pixels for both Spektr SP#1 and SP#2, and by using the ratio of corresponding lengths to determine each pitch angle. Roll and yaw, as rotated about the +XB and +ZB axes, were derived from the coordinate transformations using the pitch and CAD model coordinates. Finally, the XB component was computed directly from the coordinate transformation.

The results from this analysis were subjected to 200 iterations of a Monte Carlo error model to estimate the measurement uncertainties. The standard deviation for each input image coordinate was taken to be 0.5 pixels for each coordinate component. The resultant uncertainties expressed as one sigma (one standard deviation) are included in Table 1 along with the computed Mir coordinates (XB, YB, ZB), and the change in position from the original.

As can be seen from Table 1, the measurement errors in the XB direction are significantly higher than the errors for YB and ZB. This is to be expected due to decreased measurement accuracy along the camera optical axis. The results were visually compared with the imagery to ensure that the geometry of the damaged SP#1 made physical sense.

The limited number of views, poor camera angle, and the low resolution of the imagery accounts for most of the large measurement errors in the analysis. If additional views of SP#1

were available, the measurement accuracy along the camera optical axis would be increased. The results would likely be improved using STS-86 imagery, which show several views of SP#1 at a higher resolution.

**Table 1: Estimated Geometry of Damaged Spektr SP#1 Array**  
(Mir body coordinates)

Estimated Position with Uncertainty (inches)							Change from Undamaged Position		
Point	Xb	Xb Sigma	Yb	Yb Sigma	Zb	Zb Sigma	dXb	dYb	dZb
21	-628.9	9.9	-199.3	2.0	430.6	3.9	154.6	-41.6	38.3
22	-605.5	9.5	-330.6	1.4	446.5	4.1	131.4	-62.4	22.3
23	-573.2	7.0	-340.0	1.4	338.9	3.5	99.1	-53.1	14.9
24	-549.3	4.5	-344.5	1.2	224.5	2.9	78	-39.8	12.9
25-L	-486.6	2.1	-358.7	1.5	121.6	2.4	13	-25.9	-0.5
25-R	-494.3	2.0	-361.0	1.6	108.0	2.4	20.8	-23.6	13.2
26	-551.6	2.1	-252.3	1.6	96.4	2.1	78.3	2.8	24.6
27	-578.6	3.7	-233.7	1.8	208.6	2.6	107.6	-15.6	28.9
28	-618.8	5.6	-210.8	2.0	318.3	3.2	146.7	-30	35.5

**Appendix B: Assessment of Spektr Venting Test Imagery  
Obtained During STS-86 Fly-around**  
SN3/Space Science Branch  
Image Science & Analysis Group  
December 2, 1997

## 1. INTRODUCTION

The Spektr module was pressurized twice during the STS-86 fly-around of Mir in an attempt to detect leakage from the module. The module was ruptured in one or more places when a Progress re-supply vehicle collided with Spektr in late June of 1997. Spektr was pressurized first when the Shuttle Atlantis was crossing the +ZB axis of Mir at a distance of 240 feet, and then again when Atlantis was along the +XB axis of Mir at the same distance. Two Shuttle PLB video cameras were used to acquire views of Spektr during these pressurizations, or gas release events, to detect possible motion of the thermal insulation caused by escaping gas or to detect possible plumes which could contain debris particles. The crew also photographed Mir during the fly-around with Nikon and Hasselblad cameras. Results of the analysis of the film and video data taken during the STS-86 fly-around are presented in this report.

## 2. ACQUIRED IMAGERY

Video imagery of the Spektr module during the gas release events was obtained using a black and white Intensified Television Camera (ITVC) and a Color Television Camera (CTVC). The ITVC was mounted in the PLB B (aft port) position and the CTVC was mounted in the PLB D (forward starboard) position. The cameras were both set to an automatic exposure control and configured to have an 11 degree field-of-view containing the Solar Panel #1 attach point, the damaged radiator, and the Spektr interface to the node. Views of the events from these cameras were recorded, simultaneously, on the on-board analog Hi-8 video tapes and then transferred to digital D2 tapes after the mission. The ITVC (B camera) view is found on D2 tape 614743 (Hi-8 tape 002). The CTVC (D camera) view is found on D2 tape 614642 (Hi-8 tape 003). These tapes can be obtained from the JSC Shuttle Video Archive. The Universal Time Code (UTC) was recorded on the Hi-8 tapes and transferred to the D2 tapes, allowing accurate timing of the observed events. The quality of the CTVC view is good, however, the ITVC view suffers from a considerable amount of low-level random noise.

A review of the still photography revealed three frames of 35 mm photography (STS086-379-31,-32,-33) and three frames of 70 mm photography (STS086-720-32,-33,-34) that appear to correspond to events noted just after the first gas release. In-frame timing was not recorded on these frames, so visual comparisons with the video recordings were the only indication that the images corresponded to the video sequences.

### **3. SCREENING OF IMAGERY**

#### **3.1 Results of Video Screening**

The first gas release took place at approximately 276:19:40 UTC. Approximately one minute after this gas release, seven particles of debris can be seen moving away from the Spektr module in the CTVC view, and one particle can be seen moving from the module in the ITVC view. All these particles were observed within a 36 second time span. The second gas release took place at approximately 20:03 UTC. No debris was noted after the second gas release, and no other events, such as gas plumes emanating from the module, or the movement of insulation material, were detected during or after either of the gas release events.

The observed particles are not seen continuously as they travel through the video frames. Their intensities fluctuate rapidly, indicating that they are rotating or tumbling, and reflecting sunlight as they move through the field-of-view. The sixth particle can be seen in front of the module near the junction of Spektr and the docking node and is also seen passing in front of the Soyuz solar array. All other particles are only visible against the blackness of space. The particle seen in the ITVC view is coincident in both time and direction of travel with the seventh particle seen in the CTVC view. It is assumed that these two are the same. The other six particles could not be detected in the ITVC view, because imagery from this camera contains a larger amount of low-level video noise. Table 1 summarizes the first and last observation times of each of the particles.

#### **3.2 Results of Film Screening**

Two particles are seen in the three frames of 70 mm photography taken with the Hasselblad camera. In comparison with the CTVC view, the locations and directions of travel of these particles relative to the Spektr module suggest that they correspond to particles 6 and 7 mentioned above and listed in Table 1. High magnification of the images shows no additional detail regarding these particles in comparison with the video imagery.

A single particle was captured on three frames of 35 mm photography using the Nikon camera and a high magnification (300 or 400 mm) lens as it moved away from the module. The image contains some motion blur (probably due to the use of the high magnification lens) and may be out of focus. Only the tips of Spektr SP #1 and SP #3 are visible in these frames to indicate the particle's location. The object most likely corresponds to particle 7 listed above because of its location and brightness.

No timing from the databack was recorded on the three 70 mm frames, so they were not used to perform a trajectory analysis on the two observed pieces of debris in the film.

**Table 1. Observed Times and Estimated Speeds and Sizes of Particles**

<b>Particle Number</b>	<b>First Seen</b> (day 276:19:mm:ss.ss)	<b>Last Seen</b> (day 276:19:mm:ss.ss)	<b>Upper-Bound Size Estimate</b> (cm)	<b>Lower-Bound Speed Estimate</b> (meters/sec)
1	41:04.65	41:09.11	10	1.4 +/- 0.2
2	41:07.01	41:14.85	7	1.0 +/- 0.2
3	41:08.03	41:10.18	8	1.6 +/- 0.2
4	41:11.27	41:12.02	9	0.9 +/- 0.2
5	41:11.81	41:17.18	8	0.6 +/- 0.1
6	41:20.35	41:42.11	11	0.3 +/- 0.1
7	41:27.31	41:35.05	11	0.9 +/- 0.1
7 - ITVC	41:27.50	41:33.64	11	--

## **4. PARTICLE TRAJECTORIES, SIZE, SPEED AND POINT OF ORIGIN ESTIMATES**

### **4.1 Particle Trajectories**

Estimations for the origins of the particles can be made by tracing their trajectories. Composite images were made by combining a sequence of selected still video frames of each particle as it moved through the field-of-view. Each sequence represents a set of interim points along the trajectory of that particle. For each sequence, the first frame was chosen as the base frame and successive frames were overlaid and aligned with it using the Spektr +ZB radiator. A digital mask was then applied to the overlying frames allowing only a small region to be seen surrounding the observed particle in its new location. The resulting composite is a digital multiple-exposure showing the particle's movement.

Figures 1-5 show the composite frame-sequences that illustrate the trajectories of each of the seven particles from the CTVC camera view. Figure 8 is the ITVC (Camera B) view of particle 7. The composites have been enhanced to allow the particles to be seen in the image. Each point selected to make the composite has been circled to aid in the identification of these points.

Particles 6 and 7 have trajectories that deviate from straight-line motion. It is not certain whether this is a perspective effect caused by the motion of Atlantis around Spektr, or the result of the particles interacting either with gas leaking from Spektr or with thruster plumes coming from Atlantis or Mir. Non-linear trajectories for debris particles were noted by IS&AG on the STS-74 mission to Mir. One particle exhibited a curved trajectory over a 30-second period while the Shuttle was docked with Mir. The cause of this curvature was not investigated. Another particle exhibited a very large and instantaneous change in direction which was attributed to a Shuttle thruster firing.

### **4.2 Particle Sizes**

Analysis of the digitized video images provided an estimated upper-bound for the size of each of the seven particles. These are listed in column 4 of Table 1. The sizes were determined by plotting an intensity profile for each particle and measuring the width at the half-maximum of this profile in pixels. It was assumed the particles were at the same distance from the cameras as Spektr. Such an assumption is valid if the particles originated from the module and did not travel significantly closer to or farther from the cameras. The scale factor for converting the sizes was then derived from the known width of the Spektr +ZB radiator. The width at half-maximum of the intensity profile was used because it does not vary with the brightness of the particle and accounts for the inherent blur, or spread-function, of the video camera systems. Because it is not possible to measure sizes below this limit of resolution, and because the particles are assumed to be no closer than the module, these size measures are to be interpreted only as maximum probable size estimates.

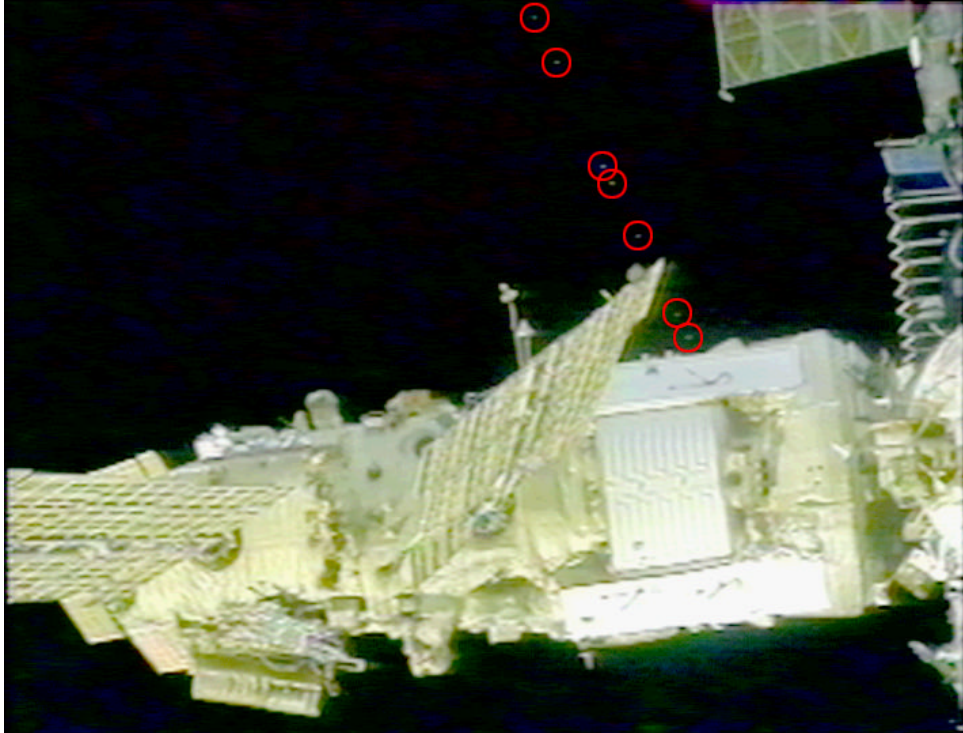


**Figure 1. Composite Image for Particle 1.**

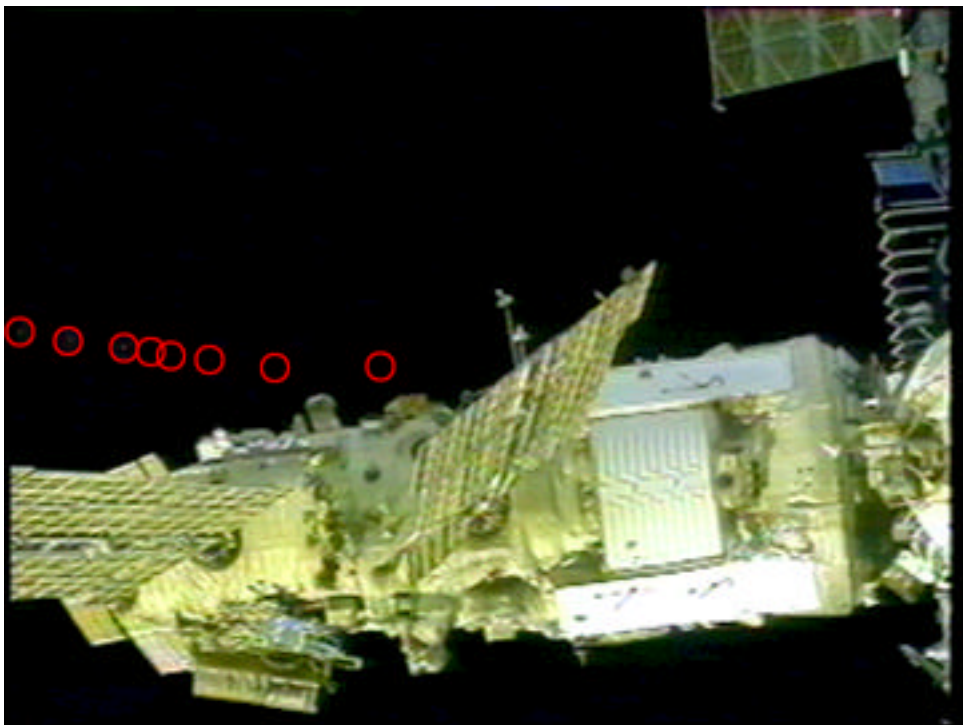


**Figure 2. Composite Image for Particle 2.**

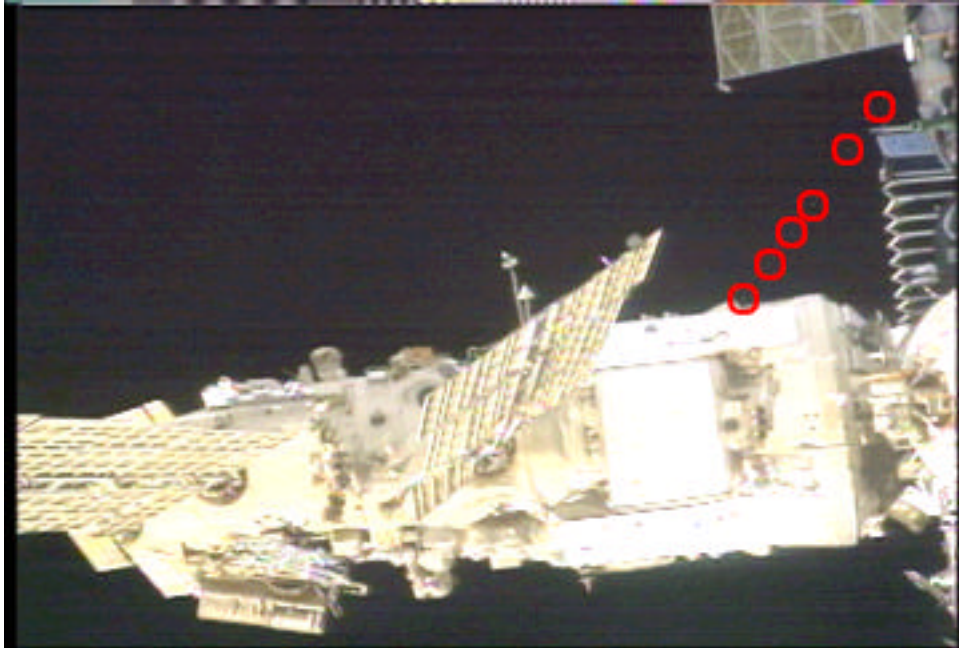


**Figure 3. Composite Image for Particle 3.**



**Figure 4. Composite Image for Particle 4.**

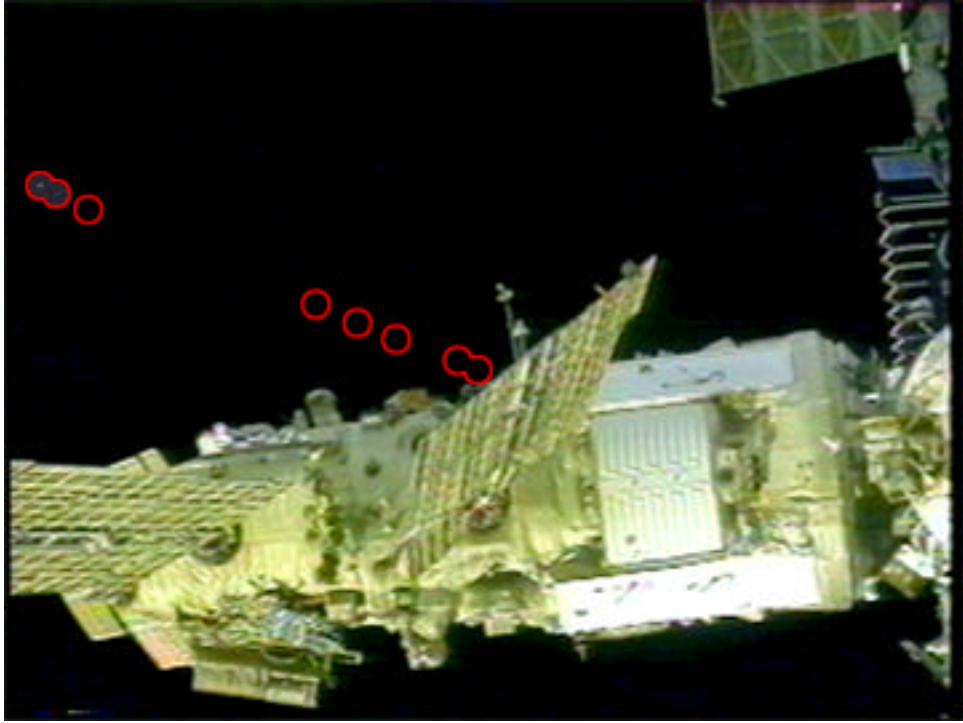


**Figure 5. Composite Image for Particle 5.**

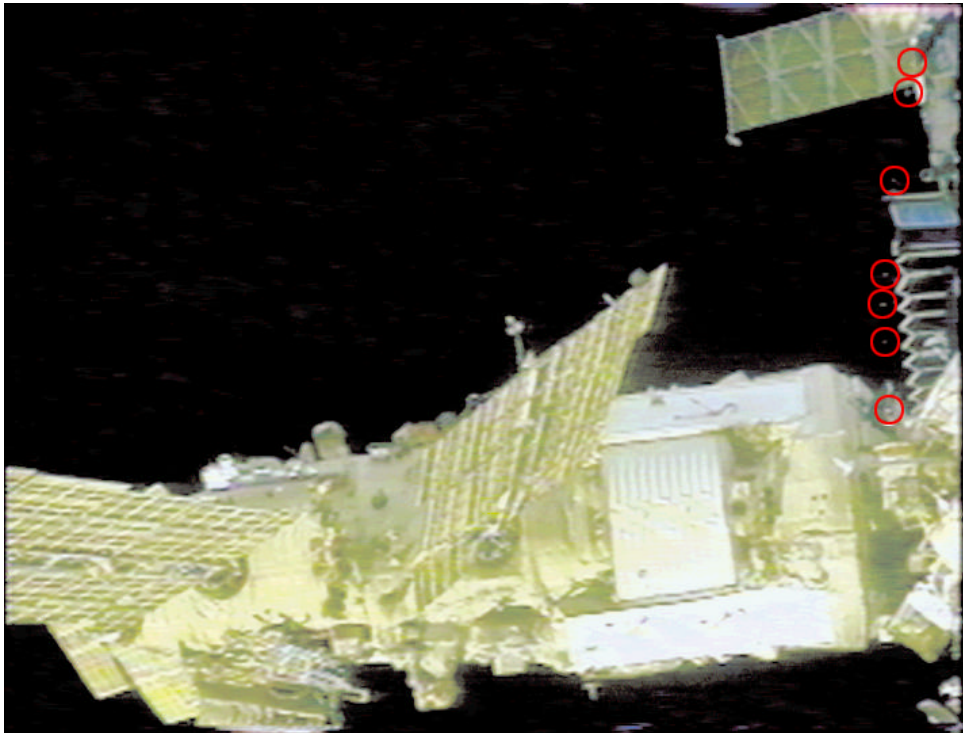


**Figure 6. Composite Image for Particle 6.**

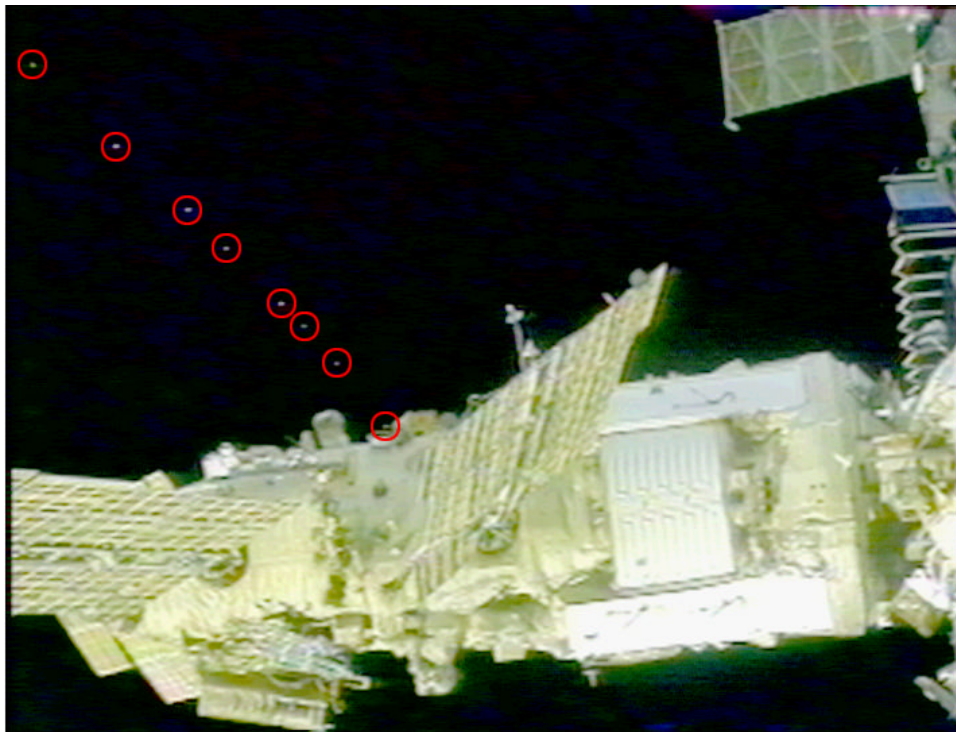


**Figure 7. Composite Image for Particle 7  
as seen from the CTVC (Camera D) view**

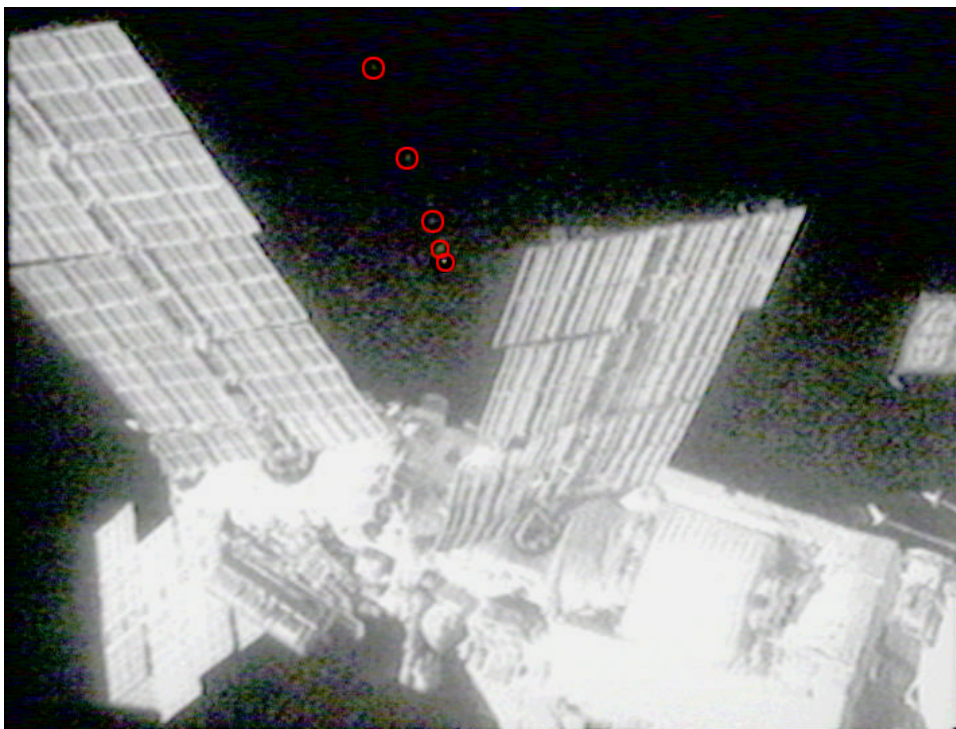


**Figure 8. Composite Image for Particle 7**

as seen from the ITVC (Camera B) view

### 4.3 Particle Speeds

To obtain an estimate for the speeds of the particles, an assumption was made that each particle was in close proximity to the Spektr module when first visible in the imagery. The apparent speed measured from the earliest two or three interim points (two in the case of particles 2, 6, and 7; three in the case of particles 1, 3, 4 and 5) were converted to an estimate for the speed of the particle using the same scale factor derived for the size estimates above. The speeds are listed in column 5 of Table 1.

Particle speeds were measured in the image plane between adjacent interim points on the composite images. For particles 1, 6, and 7, the apparent speed increased significantly. If the particles are assumed to have been traveling at a constant velocity after an initial impulse, the increases would indicate that the particles are traveling toward the camera. As the particles travel closer to the camera, they traverse a larger angle in the field-of-view per unit of time.

These calculated speeds are lower-bound estimates because only one component of each particle's velocity is being projected onto the image plane, i.e., the component that crosses the line of sight. A speed estimate was not made for particle 7 in the ITVC view, because it was visibly more clear and in closer proximity to Spektr in the CTVC view. Uncertainties in the speeds are based on a 1.5 pixel standard deviation for the x and y locations of the interim points and a standard deviation of 0.03 seconds for frame timing as a result of the conversion from SMPTE to GMT timing.

### 4.4 Particle Origins

Because there was no detection of gas plumes or the motion of insulation material near the surface of Spektr, the locations and trajectories of the seven particles observed after the first gas release serve as the only indications of where the module may be leaking. The particles do not appear to originate from the same location, suggesting that there may be more than one leak site, or that some of the particles were not related to the gas release.

A composite of the trajectories of the seven particles is shown in Figure 9. The uneven spacing of the interstitial points is a result of only choosing the brightest points in each particles trajectory for digitization. Particles one, two, three and five appear to originate from areas midway between the SP #1 attach and the junction of the module at the docking node. Particle four appears to originate from a region near the edge of the damaged thermal control system radiator panel farthest from the docking node. Particle six appears to originate from an area near the junction with the node. Particle seven appears to originate from a region stretching from the edge of the damaged thermal control system radiator panel farthest from the docking node to the scientific airlock on the -XB side of Spektr. It should be noted that this region encompasses the Spektr SP#1 attach point.

A visual comparison of the CTVC and ITVC views of the trajectory of particle seven does not reveal an origin for this particle with any greater reliability than can be determined from either of these two views alone. A three-dimensional photogrammetric analysis of these two views may yield a more conclusive result.

There is a possibility that some of the particles do not originate from the module, but are coincidentally passing through the field-of-view. Small pieces of debris have been seen on previous Shuttle-Mir missions during approach and backaway operations. Debris has also been seen during fly-around, but it is fast-moving and blurry indicating that it is in close

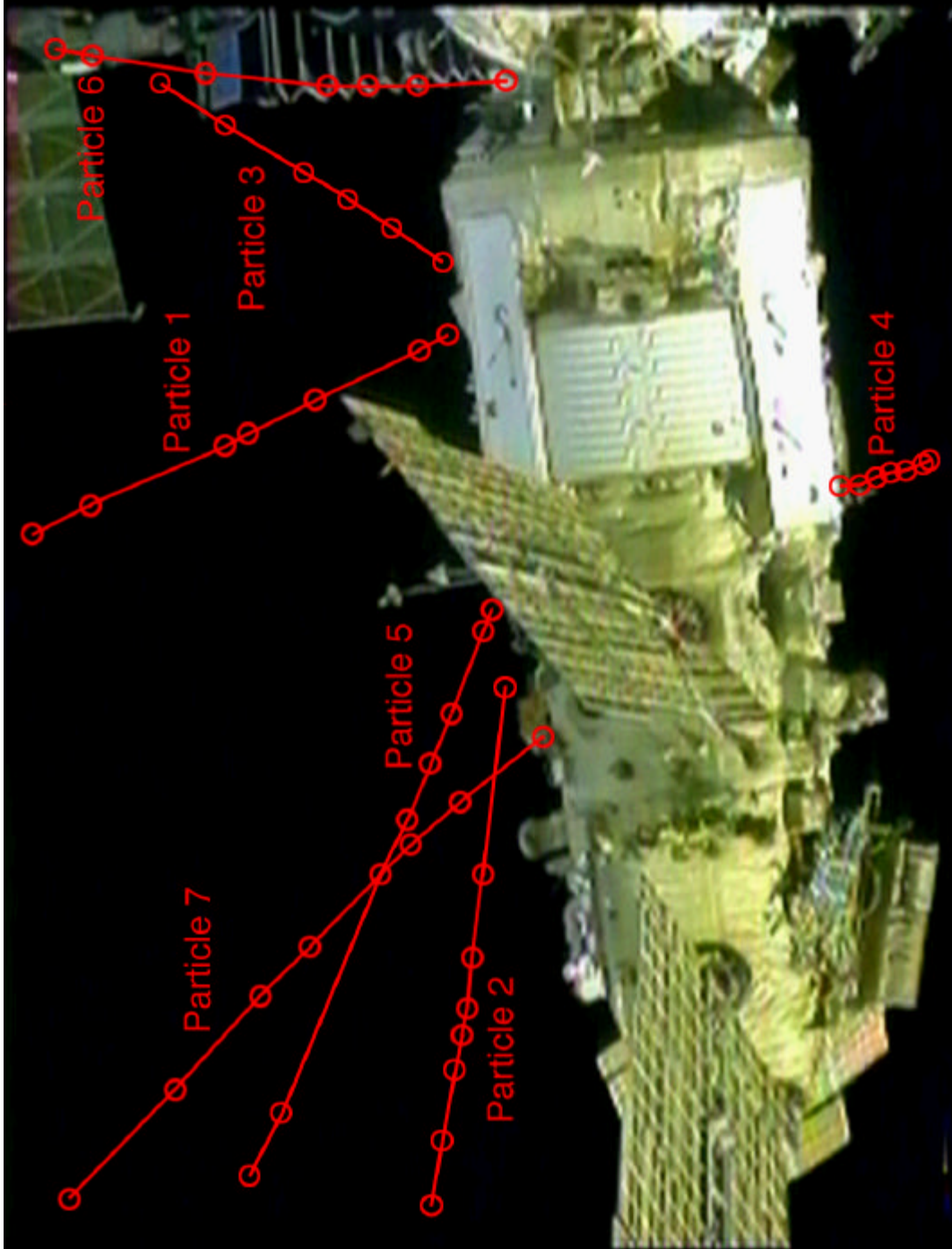


Figure 9. Composite of Particle Trajectories from CTVC (Camera D) View During Flyaround

proximity to the Orbiter. The debris noted in this report was seen within two minutes after the first gas release, and no debris was observed at any other time during the daylight portion of the fly-around (undocking and backaway for the fly-around occurred during a night pass). In addition, all of the observed particles are seen moving away from the module and never toward it, implying that they originate from somewhere on the surface of the module. Therefore, it is unlikely that these particles are randomly observed debris, but are, indeed, the result of the gas released within Spektr.

## **5. RECOMMENDATIONS**

### **5.1 Follow-on Analysis Work**

As stated above, a three-dimensional photogrammetric analysis using the two camera views may provide a precise location for the origin of particle 7. Through the application of three-dimensional photogrammetric methods, reference points in the image are used to estimate the camera location and derive a vector from that location through the object of interest, in this case, the particle at a specific moment in time. If the two views are simultaneous, the intersection of the vectors from the two views provide an estimate for the three-dimensional coordinates of the particle. The three-dimensional coordinates would need to be derived for the particle in more than one location along its trajectory for a vector to be drawn back to an intersection point with the module. The feasibility of this approach will depend on a number of factors which include the quality and quantity of available reference data, and the accuracy to which the separate views of the moving particle can be synchronized.

### **5.2 Acquisition Recommendations for STS-89**

Based on the data gathered from the STS-86 leak detection several recommendations can be made in the event that a second gas release experiment produces visible debris particles:

- The Orbiter should station-keep relative to the Mir shortly before, during, and shortly after each gas release. Station-keeping will help in the analysis of particle trajectories by providing a stable viewing perspective during the events.
- Two CTVC cameras should be used to view the module. The amount of noise contained in the ITVC signal made it less useful than expected.
- If possible, a multiplexed view (one combining simultaneous signals from two different cameras) should be recorded in addition to the normal, non-multiplexed, camera views. This would insure that, in the event that a debris particle is observed in both views, the views will be exactly synchronized. Such synchronization is necessary for a three-dimensional analysis of the trajectories of any observed debris particles. The use of multiplexed views, however, limits each camera view to only half the normal field-of-view.
- Still photography is recommended in the event gas or ice plumes form, because of the greater detail that still photography can provide. In-frame timing is required for establishing a timeline of events captured on film.

## **6. SUMMARY & CONCLUSIONS**

The video recorded from PLB camera D during the Mir fly-around on STS-86 provided data on seven particles which were seen moving away from Spektr between one and two minutes after the first gas release. One of these particles is also seen in the video recorded from PLB camera B. Two-dimensional analysis of the trajectories of the particles indicate multiple regions where the module may have leaks. Only one particle can be traced across the surface of the Spektr Module (particle 6) and only for a short distance. The current analysis has not determined precise locations of origin for the particles. Additional analysis of the imagery may yield more information.

## Appendix C: STS-86 Film Scenelist

The table below summarizes the event coverage recorded by the different still photography sources.

The attached STS-86 film scenelist was compiled by the Imagery and Publications Office/BT4 and breaks down coverage of items on each roll of 35 mm and 70 mm film.

**Table C-1 Still Photography Coverage of Mir Rendezvous Events**

	Approach	Docked (survey)	Backaway / Fly-around
<b>Hasselblad (Roll #)</b>	706	714,716,718,729	707,710,717,720,726
<b>Nikon (Roll #)</b>		301,332,334,338,341, 343,346,348,349,353, 354,365,370,371,374, 400,401,406	368,369,375,376,377, 378,379,380,381,385, 386,387,388,389,390, 392,393,394,396
<b>ESC</b>		S86E5311, S86E5313, S86E5776 thru S86E5783	

STS-86 Flight Film Contents Organized by Category, Roll, and Frame

Mag	Frames	Count	Film	Description
Category: Prime Mission Obj.				
E	5311 thru 5311	1	DIG. FILE	Mir Base Block
	5313 thru 5313	1	DIG. FILE	Damaged solar array on the Spektr module
	5776 thru 5783	8	DIG. FILE	Survey views of the Mir space station
301	006 thru 037	32	35MM CN	Survey views of the Mir space station
332	011 thru 011	1	35MM CN	Spektr module of the Mir space station
334	024 thru 024	1	35MM CN	Base Block and Kvant modules of the Mir space station
338	001 thru 037	37	35MM CN	Survey views of a Spektr solar array and radiator
340	036 thru 037	2	35MM CN	View down the length of a Spektr solar array
341	001 thru 037	37	35MM CN	Survey views of the Mir space station
343	001 thru 036	36	35MM CN	Survey views of the Mir space station
346	001 thru 036	36	35MM CN	Survey views of the Mir space station
348	001 thru 006	6	35MM CN	Strehla arm and antenna on the Mir space Station Base Block
	034 thru 036	3	35MM CN	Mir space station solar array panels
349	001 thru 025	25	35MM CN	Survey views of the Mir space station
352	001 thru 035	35	35MM CN	Survey views of the Mir space station
353	001 thru 037	37	35MM CN	Survey views of the Mir space station
354	001 thru 036	36	35MM CN	Survey views of the Mir space station
364	009 thru 010	2	35MM CN	Full Mir space station taken during approach for docking
365	001 thru 036	36	35MM CN	Survey views of the Mir space station
368	001 thru 036	36	35MM CN	Survey photos of the Mir space station
369	001 thru 038	38	35MM CN	Survey views of the Mir space station
370	002 thru 037	36	35MM CN	Survey views of the Mir space station
371	018 thru 020	3	35MM CN	Interior view of the Base Block module
	021 thru 035	15	35MM CN	Survey views of the Mir space station
372	001 thru 027	27	35MM CN	Interior views of the Mir space station
373	001 thru 001	1	35MM CN	Control board in Mir Base Block
	004 thru 036	33	35MM CN	Interior views of the Mir space station
374	013 thru 013	1	35MM CN	View of damaged Spektr module from the Mir space station
	020 thru 037	18	35MM CN	Survey views of Mir space station taken by STS-86 crew
375	001 thru 037	37	35MM CN	Survey views of the Mir space station
376	001 thru 009	9	35MM CN	Survey views of the Mir space station
377	001 thru 037	37	35MM CN	Survey views of the Mir space station
378	001 thru 037	37	35MM CN	Survey views of the Mir space station
379	001 thru 030	30	35MM CN	Survey views of the Mir space station
	034 thru 037	4	35MM CN	Survey views of the Mir space station
380	001 thru 035	35	35MM CN	Survey views of the Mir space station
381	001 thru 037	37	35MM CN	Survey views of the Mir space station
385	001 thru 012	12	35MM CN	Survey views of the Mir space station
386	001 thru 037	37	35MM CN	Survey views of the Mir space station
387	001 thru 037	37	35MM CN	Survey views of the Mir space station
388	001 thru 037	37	35MM CN	Survey views of the Mir space station
389	001 thru 037	37	35MM CN	Survey views of the Mir space station
390	001 thru 038	38	35MM CN	Survey views of the Mir space station
392	001 thru 036	36	35MM CN	Survey views of the Mir space station
393	001 thru 037	37	35MM CN	Survey views of the Mir space station
394	001 thru 037	37	35MM CN	Survey views of the Mir space station
396	001 thru 038	38	35MM CN	Survey views of the Mir space station
400	029 thru 037	9	35MM CN	Interior views of the Docking Module
401	001 thru 037	37	35MM CN	Mir solar array panels
404	025 thru 032	8	35MM CN	Interior views of the Priroda
405	010 thru 011	2	35MM CN	Soyuz spacecraft, solar array and Kvant II module
	024 thru 037	14	35MM CN	Cables and wiring in the Kristall module of the Mir space station
406	001 thru 036	36	35MM CN	Survey views of a Mir space station solar array
706	001 thru 066	66	70MM CT	Views of the Mir space station taken during approach
707	073 thru 101	29	70MM CT	Survey view of Mir space station taken after undocking
710	001 thru 045	45	70MM CT	Survey views of the Mir space station taken after undocking
712	023 thru 025	3	70MM CT	EVA tether on the end of a truss on the Mir space station
714	042 thru 098	57	70MM CT	Survey views of the Mir space station
716	000A thru 000A	1	70MM CT	Survey views of the Mir space station

STS-86 Flight Film Contents Organized by Category, Roll, and Frame

Mag	Frames	Count	Film	Description
	001 thru 067	67	70MM CT	Survey views of the Mir space station
	079 thru 098	20	70MM CT	Survey views of the Mir space station
717	047 thru 079	33	70MM CT	Survey of Spektr solar arrays and radiator
718	000A thru 000A	1	70MM CT	Soyuz spacecraft docked to the Mir space station node
	001 thru 032	32	70MM CT	Soyuz spacecraft and Travers antenna on Mir space station
720	001 thru 100	100	70MM CT	Survey views of the Mir space station
726	000A thru 000A	1	70MM CT	Survey views of the Mir space station
	001 thru 096	96	70MM CT	Survey views of the Mir space station

Prime Mission Obj. Total: 1,809

## Appendix D: STS-86 Video Scenelist Information

**Table D-1 Video Coverage of Mir Rendezvous Events**

	Approach	Docked (Survey)	Backaway / Fly-around
<b>Downlink (reel #)</b>	11,12	13,14,15,16,17,18,19, 20,21,23,24,25,26,32, 33,34,35	64,65,66
<b>Onboard (tape ID #)</b>	5,6,8,9		1,2,3,4,21,22

The above table summarizes the event coverage recorded onto the different downlink and onboard tapes. Note that some of the downlink scenes may be overlapped by those on the onboard video.

A scenelist is available for each shuttle mission, STS-1 through the present. Copies of these may be requested at the Imagery & Publications Office Customer Service Desk, Mail Code BT4, Johnson Space Center, Houston, Texas. Phone: (713) 483-7777.

## Appendix E: Sources for Report Imagery

<u>Figure #</u>	<u>Caption</u>	<u>Frame # / Tape #</u>
Cover Photo		NASA5-731-137
Figure 2.1	+ZB Fly-around Overview of the Mir Space Station	STS086-720-050
Figure 2.2	-XB Backaway Overview of the Docking Module	STS086-369-021
Figure 2.3	+XB, +ZB Fly-around Overview of Spektr	STS086-720-070
Figure 2.4	+XB, +ZB Fly-around Overview of Priroda	STS086-390-023
Figure 2.5	-XB, +ZB Fly-around Overview of Kvant-2	STS086-390-037
Figure 2.6	+ZB Fly-around Overview of Kvant / Base Block	STS086-389-017
Figure 2.7	+XB, +ZB Fly-around Overview of Progress / Kvant	STS086-388-014
Figure 3.1	+XB, +ZB Overview of Spektr Module Damage	STS086-720-069
Figure 3.2	+XB, +ZB Spektr Radiator Damage	STS086-386-014
Figure 3.3	Close-up of +XB, +ZB Spektr Radiator Damage	STS086-717-054
Figure 3.4	Cut Thermal Insulation on +ZB Surface of Spektr	STS086-389-009
Figure 3.5	+XB View of the Back Side of Spektr SP#1 and SP#3 Solar Array Damage	STS086-710-011
Figure 3.6	-XB View of the Front Side of Spektr SP#1 and SP#3 Solar Array Damage	NASA5-731-114
Figure 3.7	-ZB Overview of Spektr SP#1 Damage	STS086-368-032
Figure 3.8	Close-up of Spektr SP#1 Sheared Support Beam	STS086-717-049
Figure 3.9	Close-up of Spektr SP#1 Sheared Support Beam	STS086-386-008 (left) STS086-390-021 (right)
Figure 3.10	Close-up of Hole in Spektr SP#1	STS086-717-047
Figure 3.11	Substance on end of Kvant End Dome Purge Port	STS084-328-034 (left) STS086-392-017 (right)
Figure 3.12	Deposition on -ZB Kvant Radiator Surface	STS084-820-094 (left) STS086-714-086 (right)
Figure 3.13	Deposition on +ZB Kvant Radiator Surface	STS086-389-016
Figure 3.14	Deposition on +ZB Kvant End Dome	STS086-389-017
Figure 3.15	Solar Cells Detaching from Kvant SP#1	STS079-324-035 (left) STS086-387-017 (right)
Figure 3.16	Possible Leak on Spektr Radiator	STS086-349-011
Figure 3.17	Chipped Paint on -XB, -ZB Handrails of Spektr	STS086-714-043

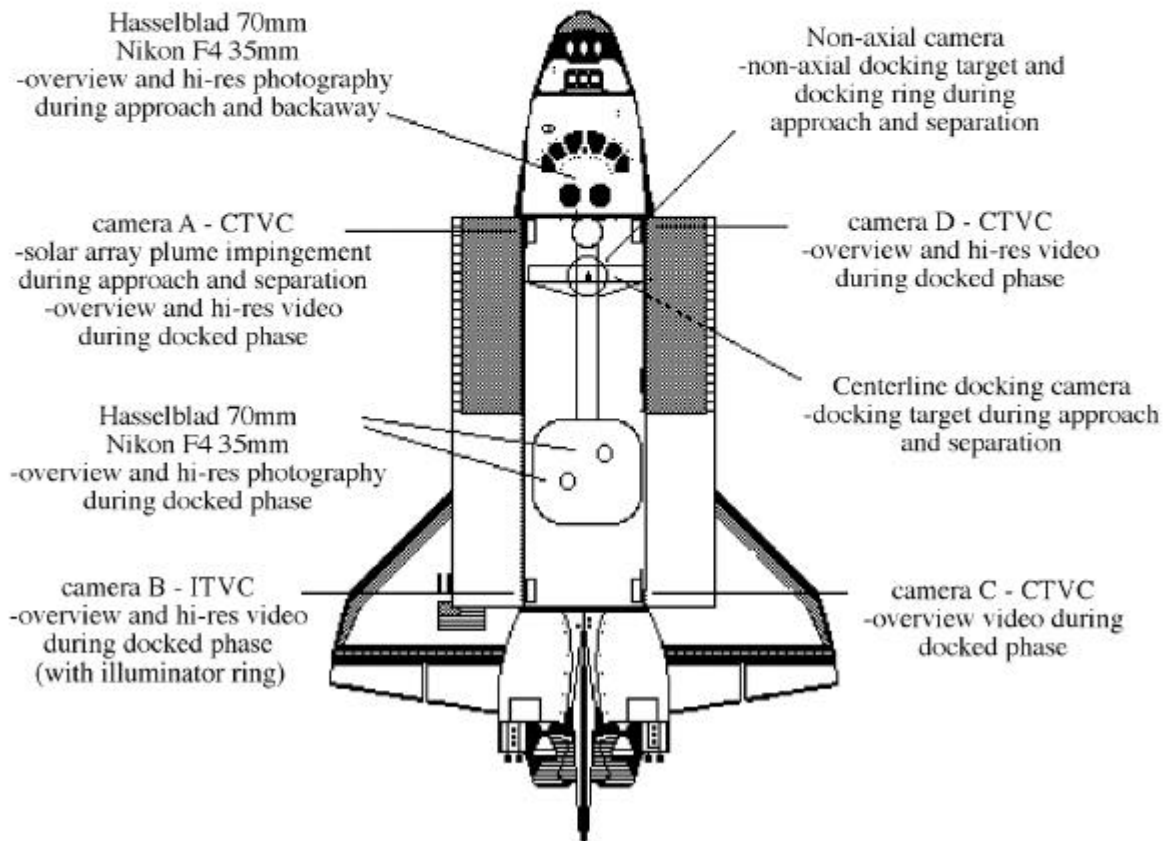
Figure 3.18	Deposition on +X Surface of OPM Thermal Blanket	STS084- (left) STS086-343-020 (right)
Figure 3.19	+ZB Discoloration and Damage on Base Block	STS086-390-005
Figure 3.20	-XB Deposition and Damage on Priroda	STS086-390-029
Figure 4.1	Photo of Docking Mechanism during Approach	STS086-706-031
<u>Figure #</u>	<u>Caption</u>	<u>Frame # / Tape #</u>
Figure 4.2	Photo of Docking Mechanism during Backaway	STS086-368-002
Figure 5.1	Representative Video Frame of CSA during Undocking	Onboard ID# 1 pt. 1
Figure 5.2	Representative Video Frames of Base Block SP#2 during Night-to-Day Transition	Tape #614682
Figure 5.3	Frame Used in the Determination of Thickness of Base Block SP#2	Tape #614682
Figure 6.1	Debris Observed Prior to Docking at GMT 270d:19h:17m:08s	Tape #614753
Figure 6.2	Debris near ODS Prior to Docking at GMT 270d:19h:41m:35s	Tape #614744
Figure 6.3	Debris after Undock at GMT 276d:17h:46m:53s	Tape #614741
Figure 6.4	Rope-like Debris noted during Station-keeping at GMT 276d:18h:11m:28s	Tape #614715
Figure 7.1	STS-86 Image of Mir with MEEP Experiments	STS086-706-031
Figure 7.2	EVA Image of PPMD (left) and ODC (right)	STS086-334-010
Figure 7.3	EVA Image of POSA II Showing Contamination	STS086-334-006
Figure 7.4	Images of the Same Section of POSA Taken on Four Separate Shuttle/Mir Missions	STS079-325-002 STS081-727-048 STS084-330-026 STS086-348-023
Figure 8.1	Kurs Antenna as seen from the Shuttle Flight Deck on STS-84	STS084-358-022
Figure 8.2	Kurs Antenna as seen from Payload Bay Camera A	Tape #614664
Figure 8.3	Kurs Antenna as seen from Payload Bay Camera D	Tape #614665

## **Appendix F: STS-86 Camera Layout**

The following diagram depicts the layout of film and photographic equipment specific to Mir survey events during the STS-86 docking.

# STS-86 Shuttle / MIR

## SURVEY CAMERA SETUP



**MIR Photo/Video Survey (DTO 1118):  
STS-86 Mission Report  
Distribution List**

CB/M. Ivins	SN3/E. Christiansen
CB/J. Wetherbee	SN3/N. Johnson
CB/S. Parazynski	SN13/K. Lulla
CB/V. Titov	SN3/M. Gaunce
CB/M. Foale	SN3/G. Byrne
C87/LMES/P. Spehar	SN3/LMES/R. Scharf (10 copies)
DA8/P. Dye	SP3/J. Maida
DF56/USA/S. Berenzweig	
DF56/USA/D. Carico	
DM34/S. Dunham	YA/F. Culbertson
DO451/G. Schneider	YA/D. Hanson
DT23/USA/G. Hennington	YA/J. Van Laak
EA/T. Farrell	HQ/ID/R. Baldwin
ES2/J. Dagen	HQ/XS/D. Brewer
B30/LMES/Q. Tran	HQ/MOC/G. Kirkham
ES5/J. McManamen	HQ/MZ/C. Lively
HS-23/MDA/C. Soares	HDQS/ML/M. Swilley
MA/T. Holloway	HQ/QP/Miles Whitnah
MA2/J. Williams	KSC/TV-MSD-7/G. Katnik
MA3/J.D. Holt	MDC2-3352/T. Bartkowicz
MS2/G. Lange	MSFC/EL23/B. Kauffman
MS3/B. Brown	MSFC/EP24/T. Reickhoff
MT3/G. Buoni	B30/LMES/B. Rochon
MV5/R. Edmiston	
NS3/K. Scott	
OA/R. Brinkley	Gabe Katell
OA/K. Chilton	Rocketdyne Division
OB/BOE/D. Winfield	Rockwell International
OH/J. Nise	Mail Code LA70
OM/M. Geyer	6633 Canoga Ave.
OM/HS40/G. Ulrich	P.O. Box 7922
OZ/R. Suggs	Canoga Park, CA 91309-7922
OZ2/C. Statham	
OZ2/R. Lofton	Michael D. Bjorkman
OZ2/Dynacs/C. Conley	Boeing Defense & Space Group
BT53/JSC Library (5 copies)	P.O. Box 240002
BT533/Space Station Library (5 copies)	Huntsville, AL 35824-6402
SA/J. Loftus	
SA/R. Nygren	William Kinard
SM3/G. Kitmacher	Mail Stop 188B
SN/D. Blanchard	NASA Langley Research Center
SN/D. Thompson	Hampton, VA
SN2/F. Horz	

Greg Stover  
Mail Stop 356  
NASA Langley Research Center  
Hampton, VA

Hyoung-Man Kim  
Mail Stop JHOU-2520  
13100 Space Center Blvd.  
Houston, TX 77059-3556

Thomas W. Kerslake  
Mail Stop 500-203  
NASA Lewis Research Center  
21000 Brookpark Rd.  
Cleveland, Ohio 44135